國 立 交 通 大 學

生物科技研究所

碩 士 論 文

克雷白氏肺炎桿菌 CG43 中參與莢膜多醣體生合成之核心蛋白 Wza、Yor5、Yco6 和 Wzx 的功能性研究

Functional analysis of the core elements, Wza, Yor5, Yco6 and Wzx, involved in capsular polysaccharide biosynthesis in *Klebsiella pneumoniae* CG43

研 究 生： 李智凱

學 號： 9328507

指導教授：彭慧玲 博士

中華民國九十五年七月

中文摘要

克雷白氏肺炎桿菌為一株伺機性引起區內感染疾病的格蘭氏陰性菌，其外部包覆著由多醣體所組成的厚莢膜。此一莢膜可以讓細菌逃避細胞的吞噬作用以及避免被血清因子所毒殺。克雷白氏肺炎桿菌的莢膜多醣體被認為和大腸桿菌的第一類莢膜多醣體之生合成與組合途徑相類似，由位於 *cps* 基因組中的主要因子所調控，這些主要因子包括了 Wzi、Wza、Yor5、Yco6、Wzx 和 Wzy。本研究的主要目標為證明其中四個主要因子－Wza、Yor5、Yco6 和 Wzx－的生物功能性。在實驗室之前的研究中，證明了無論剔除酪胺酸去磷酸酶或是酪胺酸激酶的基因，*yor5* 或 *yco6* 皆會明顯地減少其原本所具有的黏性和莢膜多醣體的量。在此研究之中，我們亦構築了剔除了 *wza* 或 *wzx* 的突變株。其中剔除了位在外膜上的多醣體輸送蛋白 *wza*，會使得莢膜多醣體之聚合體無法運送到細菌表面，並且進而回饋抑制上游的生合成途徑，造成整體生成量明顯地下降。而在 *wzx* 突變株之中，雖然莢膜多醣體的總量同樣下降，但是仍然有少量的聚合體存在，這部分的多醣體合成作用可能不需要經由 Wzx 來調控。此外，剔除 *yor5* 和剔除 *yco6* 這兩個突變株皆完全地喪失了莢膜多醣體的聚合體，而這也證明了由 Yco6 和 Yor5 所調控的酪胺酸磷酸化作用對於莢膜多醣體的生成與聚合作用來說相當重要。經由體外磷酸化試驗，我們證實了克雷白氏肺炎桿菌和大腸桿菌的蛋白質酪胺酸激酶－Yco6 和 Wzc－都能夠將克雷白氏肺炎桿菌中的 Ugd、Gnd、ManB 和 ManC 這四個酵素磷酸化，而這些酵素和莢膜多醣體醣類核甘酸前驅物的生成相關。而 Ugd 和 Gnd 的磷酸化對於其酵素活性則有明顯的提升效果。另外，以蛋白質酪胺酸去磷酸酶 Yor5 來進行體外去磷酸化試驗則發現，Gnd 和 ManC 可以徹底地去磷酸化，而 KpUgd 則是部分被去磷酸化。相反地，ManB 則是完全不受 Yor5 影響。以上實驗結果明確地證實了這些主要因子對於克雷白氏肺炎桿菌的莢膜多醣體之生合成與組合作用的重要性和其功能性角色。

Abstract

Klebsiella pneumoniae, an opportunistic gram-negative bacterium causing community-acquired diseases, are mostly encapsulated by a considerable thick polysaccharidic capsule acting to protect the bacteria from phagocytosis and prevent from killing by serum factors. The capsular polysaccharide (CPS) is made from a similar biosynthetic and assembly pathway to that of *Escherichia coli* group 1 CPS. The core elements encoded in *cps* gene cluster include Wzi, Wza, Yor5, Yco6, Wzx and Wzy. Our previous study has demonstrated that deletion of either *yor5*, encoding a protein-tyrosine phosphatase, or *yco6*, coding for a protein-tyrosine kinase, in *K. pneumoniae* CG43 reduced significantly the bacterial mucoidy and CPS content. In this study, both *wza*$^-$ and *wzx*$^-$ mutants were generated and the deletion effects were analyzed and compared. Deletion of *wza*, encoding an outer membrane polysaccharide export protein, or *wzx*, coding for a flippase, appeared to affect also the mucoidy and reduce the CPS content. Polymeric CPS were blocked in periplasma in *wza*$^-$ mutants and resulted in feedback inhibition of total CPS synthesis. In contrast, some polymeric CPS was observed on cell surface in the *wzx*$^-$ mutant suggesting an alternative translocation system for oligosaccharides through the cytoplasmic membrane. Nonetheless, to demonstrate further a role of tyrosine phosphorylation, several recombinant clones were generated and the proteins, including Yor5, Yco6, Ugd, Gnd, ManB and ManC that have been shown to be required for regulation and synthesis of CPS sugar nucleotide precursors, were purified. Via *in vitro* phosphorylation assay, the recombinant Yco6 appeared to be able to phosphorylate the enzymes Ugd, Gnd, ManB and ManC, and the phosphorylation increased the enzymatic activities of Ugd and Gnd. Moreover, the phosphorylated Ugd, Gnd and ManC, but not the ManB, could be dephosphorylated by the recombinant Yor5.

致謝

很快地，碩士班生涯的兩年時光就這樣過了。還記得剛進入這個實驗室的我，仍是個對於「做研究」這門學問絲毫不懂的大學畢業生，經過了在實驗室之中的訓練、老師的指導，以及學長姊們的幫助之下，才得以完成這個論文的內容。在這段期間認識了很多人，學到了許多東西，接觸了很多事物，所經歷的一切一切都要感謝身邊的大家，有你們才會有現在的我和這篇論文。首先要感謝彭老師，帶我進入這個實驗室和細菌學這個領域，一路上給予我指導和幫助，並且提供了一個良好的研究環境，以及相當自由的研究空間，才能夠讓我有這樣的研究成果；感謝鄧文玲老師和邱顯泰老師，百忙之中撥空來擔任我的口試委員，並且提供了我論文上許多相當寶貴的建議；感謝已經畢業的平輝學長，常常在工作之餘抽空來關心我的實驗進度，且不厭其煩地回答我提出的實驗問題，讓我能夠在一開始時可以容易地進入狀況；感謝實驗室的靖婷、盈蓉學姊和新耀、健誠學長，在實驗上帶我操作許多實驗、提供許多想法、給予很多幫助與建議，讓我得以順利完成實驗，在生活上陪伴我的喜怒哀樂，讓我研究之外的生活也能過的充實；感謝和我同屆的育聖和心瑋同學，很開心能夠和你們一起度過碩士班的這兩年；感謝實驗室的登魁、格維、朝陽這幾個學弟，已畢業的祐俊學長，還有可愛的專題生們，在各方面的照顧；感謝其他實驗室的阿男、玉淳、琮道、媛婷、程翔等學長姊，以及所有在這段期間認識的各位，認識你們真好；感謝我的家人，無怨無悔地在背後默默支持我，讓我順利地完成碩士班學業。最後在這邊要特別感謝提供了我大腸桿菌Wzc和Ugd蛋白表現載體的Christophe Grangeasse博士，讓我的實驗能夠有所進展。

Contents

Table contents

Page

Figure contents

Page

Abbreviation

ABC	ATP-binding cassette
ATP	adenosine triphosphate
BCIP	5- bromo-4-chloro-3-indolyl phosphate
bp	base pair
CFU	colony forming unit(s)
CIAP	calf intestine alkaline phosphatase
CPS	capsular polysaccharide
DOC	deoxycholic acid
DNA	deoxyribonucleic acid
EDTA	ethylenediamine-tetraacetic acid
EPS	exopolysaccharide
GDP	guanosine 5'-diphosphate
IPTG	isopropyl-1-thio-β-D-galactopyranoside
kb	kilobase(s)
kDa	kiloDalton(s)
LB	Luria-Bertani
mRNA	messenger RNA
NAD	nicotinamide adenine dinucleotide
NADH	nicotinamide adenine dinucleotide (reduced form)
NBT	nitro blue tetrazolium chloride

ORF	open reading frame
PAGE	polyacrylamide gel electrophoresis
PBS	phosphate buffered saline
PCR	polymerase chain reaction
PPP	pentose phosphate pathway
PTK	protein-tyrosine kinase
PTP	protein-tyrosine phosphatase
PVDF	polyvinylidene difluoride
RNA	ribonucleic acid
rpm	revolutions per minute
RT-PCR	reverse transcriptase-PCR
SDS	sodium dodecyl sulfate
TEM	transmission electron microscopy
UDP	uridine 5'-diphosphate
und-PP	undecaprenyl diphosphate

Introduction

Klebsiella pneumoniae, a member of the *Enterobacteriaceae*, is a rod-shaped and opportunistic gram-negative bacterium. It can cause community-acquired diseases including pneumonia, bacteremia, septicemia, urinary tract and respiratory infections, occurring particularly in immunocompromised patients (Podschun and Ullmann, 1998). Most *Klebsiella* strains are encapsulated by a polysaccharidic capsule of considerable thickness responsible for the glistening and mucoid colonies on agar plates. The highly virulent clinical isolates are often carry heavy capsules as an important virulence factor to protect the bacteria from phagocytosis and prevent from killing by serum factors (Simoons-Smit *et al.*, 1986).

The capsular serotypes of *Klebsiella* strains have been classified as 77 K antigens (Ørskov and Ørskov, 1984). On the basis of mouse lethality assay, the strains belonging to serotypes K1 and K2 were found to be the most virulent (Simoons-Smit *et al.*, 1986). *K. pneumoniae* CG43, showing a strong virulence to Balb/c mice with 50% lethal dose of 10 CFU, is a highly encapsulated clinical isolate of K2 serotype (Chang *et al.*, 1996). The structure of *K. pneumoniae* K2 capsular polysaccharides (CPS) has been determined as [→)4-Glc-(1→3)-α-Glc-(1→4)-β-Man-(3←1)-α-GlcA)-(1→]$_n$ (Wacharotayankun *et al.*, 1992), which is made from a similar biosynthetic pathway to that of *Escherichia coli* group 1 CPS (Whitfield and Roberts, 1999).

On the basis of genetic and biosynthetic criteria, CPS in *E. coli* has been classified into four different groups. These include two fundamentally different polymerization pathways. Group 1 and 4 CPS follow a Wzx/Wzy-dependent polymerization pathway, in which undecaprenol diphosphate (und-PP)-linked repeat units are formed at the

inner leaflet of the inner membrane. These und-PP-linked intermediates are flipped across the membrane by a process involving Wzx protein and then polymerized in a reaction requiring Wzy. Group 2 and 3 CPS are assembled by an ABC (ATP-binding cassette)-transporter-dependent pathway, in which und-PPlinked polymers are formed at the inner leaflet of the membrane by processive glycosyltransfer to the nonreducing terminus of the und-PP-linked intermediate. The nascent polymer is then exported across the inner membrane by an ABC transporter (Whitfield, 2006).

In terms of primary structure and mechanism of synthesis, the *Klebsiella* capsules resemble those of *E. coli* group 1 and, in some cases, same polymer structures are found. In *E. coli*, the genes for group 1 CPS synthesis and translocation were characterized as the core elements including *wzi*, which is involved in surface assembly of CPS and acts as an anchor of CPS; *wza*, which encodes a polysaccharide export protein; *wzb*, encoding a low-molecular-weight phosphatase; *wzc*, encoding a protein-tyrosine autokinase; *wzx*, encoding a flippase responsible for oligosaccharides translocation; and *wzy*, encoding putative polymerase (Drummelsmith and Whitfield, 1999).

The gene cluster *cps* (capsular polysaccharide synthesis) region that is responsible for K2 CPS synthesis of *K. pneumoniae* Chedid has been determined, which contains a total of 19 open reading frames (ORFs) organized into 3 transcriptional units (Arakawa *et al.*, 1995). Among these genes, *orf3* to *orf6*, a highly conserved four-gene-block, are counterparts of *E. coli wzi-wza-wzb-wzc* (Rahn *et al.*, 1999). Wzi, an *orf3* encoding protein, is an outer membrane protein and *wzi* mutant showed a significant reduction in cell-bound CPS polymer with a corresponding increase in cell-free material. This proposed that Wzi plays a late role in capsule assembly, perhaps in the process that links high-molecular-weight capsule to the cell surface

(Alvarez *et al.*, 2000; Rahn *et al.*, 2003). *orf4* encodes for a Wza homolog, *orf5* for Yor5, and *orf6* for Yco6, respectively. Enzymatic activities of the two proteins, Yor5 and Yco6, which are respectively Wzb and Wzc homolog, have been demonstrated. Similar to the *E. coli* Wzb and Wzc, Yor5 is a protein-tyrosine phosphatase (PTP) and Yco6 is a protein-tyrosine kinase (PTK) (Preneta *et al.*, 2002). The *orf10* encodes a membrane protein containing multi-transmembrane domains, which is likely the homolog of *E. coli* Wzy, and the *orf11* is likely the *wzx* homolog, which encoding a flippase involved in the export of antigen out to cell surface (Paulsen *et al.*, 1997).

Among these core elements, PTK and PTP are assumed to regulate the tyrosine phosphorylation in the cells. Phosphorylation is a covalent modification that proteins frequently undergo in a post-translational process. Protein phosphorylation on tyrosine is one type of phosphorylation that was long considered to be specific in eukaryotes, which has been shown to be critical in the regulation of a series of fundamental biological functions, including signal transduction, growth control, and malignant transformation (Hunter, 1995). Comparing to the eukaryotic systems, less is known about the physiological roles of protein-tyrosine phosphorylation in bacteria. The first indication of a PTK activity in bacteria has been reported in *E. coli* (Manai and Cozzone, 1983). Nevertheless, the first bacterial PTK, Ptk, an 81 kDa protein located in the inner-membrane fraction, was identified in *Acinetobacter johnsonii*, which is able to autophosphorylate on multiple tyrosine residues at the expense of ATP (Duclos *et al.*, 1996; Grangeasse *et al.*, 1997). In recent years, several homologous PTKs were reported in other Gram-negative and Gram-positive bacteria, including AmsA from *Erwinia amylovora* (Bugert and Geider, 1997), Yco6 from *K. pneumoniae* (Preneta *et al.*, 2002), EpsB from *Pseudomonas solanacearum* (Huang and Schell, 1995), ExoP from *Sinorhizobium meliloti* (Niemeyer and Becker, 2001),

CapB from *Staphylococcus aureus* (Lin *et al.*, 1994), Waap from *Pseudomonas aeruginosa* (Zhao and Lam, 2002), and CpsC from *Streptococcus pneumoniae* (Morona *et al.*, 2000). In addition, bacteria often contain PTPs simultaneously, which antagonize the activity of PTKs. The genes encoding PTKs and PTPs are generally located in the gene clusters involved in biosynthesis and transport of CPS or exopolysaccharides (EPS) (Vincent *et al.*, 1999).

Together, PTKs and PTPs play important roles in the production and processing of CPS and EPS (Nakar and Gutnick, 2003; Stevenson *et al.*, 1996). In *E. coli*, knock-out of PTK or PTP corresponding genes, *wzc* or *wzb*, apparently reduced the production of CPS and colanic acid (Vincent *et al.*, 2000). In *S. pneumoniae*, autophosphorylation of CpsD kinase decreased its activity which consequently lowered the production of CPS (Morona *et al.*, 2000). The question as to how the regulation affects CPS biosynthesis via tyrosine phosphorylation remains elusive. Recently, a growing number of protein substrates of the PTKs have been reported, which include RNA polymerase heat shock sigma factors in *E. coli* (Klein *et al.*, 2003), UDP-glucose dehydrogenases in *E. coli* and *Bacillus subtilis* (Grangeasse *et al.*, 2003; Mijakovic *et al.*, 2003), and single-stranded DNA-binding proteins in *B. subtilis* (Mijakovic *et al.*, 2006). Phosphorylation of these proteins appeared to enhance their activities and hence promoted respectively the biological functions.

In the *cps* gene cluster of *K. pneumoniae* Chedid, besides the PTK and PTP encoding genes, other *cps* genes encoding glycosyltransferases or enzymes for producing sugar nucleotide precursors are designated to CPS synthesis include *gnd*, *manC* and *manB*. Gnd is 6-phosphogluconic dehydrogenase involving in pentose phosphate pathway (PPP), which catalyzes the oxidative decarboxylation of 6-phospho-gluconate to ribulose-5-phosphate. In *E. coli*, PPP is a major route for

intermediate carbohydrate metabolism and plays various roles, including breakdown of carbon sources, generation of reducing power (NADPH) and essential metabolites for biosynthesis, and formation of the components of polysaccharide layer of the cell. Furthermore, Gnd is involved in the metabolism of glucose and gluconate and generally exists in enterobacteria (Sprenger, 1995). GDP-mannose pyrophosphorylase and phosphomannomutase encoded respectively by *manC* and *manB* are required for the formation of GDP-mannose, a precursor required for the formation of both CPS and LPS (Jayaratne *et al.*, 1994). As shown in Fig. 2, ManC, ManB, and Gnd proteins are apparently involved in the biosynthesis of CPS repeat units.

In this work, the goal is to demonstrate the biological roles of Wza, Yor5, Yco6, and Wzx by generation of the specific gene deletion mutants and analyses of the mutant phenotypes. In addition, I examined the possibility whether Gnd, ManC, ManB, and Ugd of *K. pneumoniae* CG43 are the substrates of the PTK Yco6 and the PTP Yor5, and if the phosphorylation and dephosphorylation are able to modulate their enzymatic activities.

Materials and methods

Bacterial strains, plasmids, and growth conditions. The bacterial strains and plasmids used in this study are listed in Table 1 and Table 2 respectively. The genomic DNA for PCR amplification was prepared from *K. pneumoniae* CG43, a liver abscess isolate of K2 serotype recovered from Chang Gung Memorial Hospital, Linkou, Taiwan. All bacteria were propagated at 37℃ in Luria-Bertani (LB) broth supplemented with appropriate antibiotics when needed including kanamycin (25 μg/ml), ampicillin (100 μg/ml) , tetracycline (20 μg/ml) and streptomycin (500 μg/ml). The plasmids, pQE30-41, pQE30-42 and pQE30-U, are gifts from Institut de Biologie et Chimie des Prote´ines, France (Grangeasse *et al.*, 2003).

DNA manipulation. Plasmids were purified by using the High-Speed Plasmid Mini kit (Geneaid, Taiwan). All restriction and DNA-modifying enzymes were used as recommended by the manufacturer (Fermentas, USA). PCR amplifications were performed with Taq DNA polymerase (MDBio, Inc, Taiwan). PCR products and DNA fragments were purified using the Gel/PCR DNA Fragments Extraction kit (Geneaid, Taiwan). The primers used in this study were synthesized by MDBio, Inc, Taiwan. Transformation of *E. coli* cells was performed by following the method of Dower (Dower *et al.*, 1988).

Construction of the specific gene-deletion mutants and complements. *K. pneumoniae* CG43 mutants disrupted specifically at *yor5*, *yco6*, *wza*, or *wzx* genes were constructed by the allelic exchange strategy. The primer sets used for PCR amplification of the DNA fragments flanking sequence are listed in Table 3. The generated DNA fragments were cloned into pKAS46, a suicide vector (a generous gift

from Dr. Skorupski, University of New Hampshire), and the resulting plasmids were then mobilized to *K. pneumoniae* CG43-S3 through conjugation from *E. coli* S17-1 λ *pir*. The trans-conjugants were selected with kanamycin on minimal medium (M9 minimal salts, Sigma). Some of the kanamycin-resistant transconjugants was picked and then spread onto a LB plate supplemented with streptomycin. When the occurrence of a double cross-over, the streptomycin-resistant and kanamycin-sensitive colonies were isolated, and the deletions of *wza*, *yor5*, *yco6*, and *wzx* were verified by PCR and by Southern blot analysis with a gene specific probe. To obtain the complement of *wza*, *yor5*, *yco6* and *wzx*, the genes were amplified from *K. pneumoniae* CG43-S3 with the primers listed in Table 3 and the DNA fragment was ligated into pRK415, a broad host range plasmid (Keen *et al.*, 1988).

Quantification of the glucuronic acid content. The CPS was extracted by using the method described previously (Domenico *et al.*, 1989). Briefly, bacteria were collected from 500 μl of overnight culture and mixed with 100 μl of 1% Zwittergent 3-14 detergent (Sigma-Aldrich, Milwaukee, WI) in 100 mM citric acid (pH 2.0). The mixture was incubated at 50℃ for 20 min. After centrifugation, 250 μl of the supernatant was transferred to a new tube and CPS was precipitated with 1 ml of absolute ethanol. The pellet was then dissolved in 200 μl distilled water and a 1200 μl of 12.5 mM borax (Sigma-Aldrich, Milwaukee, WI) in H_2SO_4 was added. The mixture was vigorously vortexed and boiled for 5 min, subsequently cooled on ice. Then 20 μl of 0.15% 3-hydroxydiphenol (Sigma-Aldrich, Milwaukee, WI) was added and the absorbance at 520 nm was measured. The uronic acid content was determined from a standard curve of glucuronic acid (Sigma-Aldrich, Milwaukee, WI) and expressed as μg per 10^9 CFU.

Bacterial fractionation. Cell pellet was collected from 5 ml of overnight culture, and washed three times with STE buffer (10mM Tris-HCl, pH 7.5, 10mM EDTA, 25% sucrose). After centrifugation, the pellet was resuspended in 0.4 ml ice-cold water and proceeded with osmotic shock (put on ice for 10 min and subsequently stand at 37℃ for 10 min, repeat three times). After centrifugation at 12000 ×g for 5 min, the supernatant was assigned as the periplasmic fraction, and the pellet resuspended in 0.4 ml T buffer (50mM Tris-HCl, pH 8.0, 30mM magnesium acetate, 2mM dithiothreitol). After disruption by sonication and centrifugation at 180000 ×g for 60 min, the supernatant and pellet were collected as the cytoplasmic fraction and membrane fraction, respectively.

Analysis of the capsular polysaccharide. Capsular polysaccharides were purified as described (Whitfield *et al.*, 1992). Briefly, cells were harvested from overnight culture and pelleted at 13200 rpm for 10 min. The pellet was resuspended in 500 µl PBS and extracted with hot-phenol, and then dialyzed against water overnight. The crude extract was treated with DNase (4 mg/ml), RNase (0.2 mg/ml) and proteinase K (4 mg/ml) and dialyzed against water. The extracted CPS was then analyzed by 5% or 10% DOC-PAGE. After electrophoresis, the gel was immediately immersed in 100 ml of alcian blue solution (0.005% alcian blue, 40% ethanol, 5% acidic acid) and gently rocked for 30 min as described (Reuhs *et al.*, 1998). This was followed by a change to 100 ml of fresh solution and overnight rocking. The gel was then rinsed for 5 min in dH_2O and oxidized in 100 ml of 0.7% sodium metaperiodate for 10 min, and washed five times in 200 ml of dH_2O for 5 min each time. After the gel was stained in 100 ml of silver solution (10% Bio-Rad silver concentrate) for 10 min and rinsed in dH_2O for 5 min, 100 ml of developer (Bio-Rad) was added with agitation until dark precipitate formed and immediately drained to remove all precipitate. Finally, the color was

developed with developer again for 5 min. The development was stopped by 100 ml of 5% acetic acid for 10 min followed by a rinse of 200 ml dH_2O.

Visualization of the CPS by electron microscopy. As described by Reid (Reid and Whitfield, 2005), the cells were grown to mid-exponential phase in LB broth containing the appropriate antibiotics. The cultures with an optical density at 600 nm of about 0.5 were collected by centrifugation at 5,600 ×*g* for 5 min. The cells were washed twice with 0.5 ml of phosphate buffered saline (PBS) and the pellets were incubated with 20 µl cationized ferritin solution (Sigma F-7879) for 30 min at room temperature with gentle agitation. Binding of the cationized ferritin binds to negatively charged capsule prevents it from dehydration for analysis by electron microscopy. Finally, the cells were collected by centrifugation and washed twice with 0.5 ml of PBS to remove the unbound ferritin and then processed for visualization by transmission electron microscopy (JEOL JEM 2000EXII).

Polymyxin B sensitivity assay. The Polymyxin B sensitivity assay was performed by using the method described (Campos *et al.*, 2004). Cells were grown at 37°C in LB medium and harvested at the exponential phase of growth, and a suspension containing approximately 10^5 CFU/ml was prepared in 1% (wt/vol) tryptone-PBS (pH 7.4). Then, 100 µl of the cell suspension was mixed with various concentrations of polymyxin B in a volume of 1 ml, followed by incubation at 37°C for 30 min. Finally, 100 µl of the suspension was plated on LB agar plates and the plates were incubated overnight at 37°C for colony formation. The colony counts were determined and expressed in percentage to the colony counts of bacteria not exposed to polymyxin B.

Biofilm formation assay. The measurement of biofilm formation was performed according to the method described (O'Toole and Kolter, 1998). Overnight grown

bacteria were diluted (1:100) in culture medium, and 100 μl diluted bacteria were inoculated into each well of a 96-well microtiter dish (TPP industries, France) and incubated at 37°C for 48 h to allow the formation of biofilm. After incubation, each well was washed with water and 150 μl of 1% crystal violet was added for incubation at room temperature for 30 min. Subsequently, after washing with water, 150 μl of 1% SDS was added to each well and the microtiter dish was shaken to dissolve the dye. The capability of biofilm formation was quantitated by determining absorbance at 595 nm and each biofilm result represented the mean of three separate experiments.

Western immunoblotting. The purified proteins were analyzed by SDS-PAGE and the resolved proteins were transferred to a polyvinylidene difluoride (PVDF) membrane electrophoretically in the transfer buffer containing 137 mM NaCl, 2.7 mM KCl, 10 mM Na_2HPO_4, 2 mM KH_2PO_4 and 20% methanol. The His_6-tagged proteins were detected by anti-His-tag monoclonal antibody (Novagen) and phosphotyrosine proteins were detected by anti-phosphotyrosine monoclonal antibody (Sigma P4110). The secondary antibody, an anti-mouse IgG conjugate alkaline phosphatase antibody (Sigma), was then applied and the bound complex was detected by using nitro blue tetrazolium chloride (NBT)/5-bromo-4-chloro-3-indolyl phosphate (BCIP) as the substrates.

Constructions of the recombinant His_6-tagged proteins. For construction of the kinase domain expression plasmid pET30-Yco6E23, 0.85-kb DNA fragment of *yco6* (from nucleotide 1351 to 2166), which encoding the C-terminal PTK domain of Yco6, was PCR-amplified from *K. pneumoniae* CG43-S3 using the primer pair Yco6E2 and Yco6E3 (Table 3). The DNA fragment was restricted by *Eco*RI/*Sal*I and then ligated into pET-30b vector, which resulting of the plasmid pET30-Yco6E23. To generate other recombinant plasmids including pET30-Yor5, pET30-Ugd, pET30-Gnd,

pQE31-ManC and pQE31-ManB, the respective coding region of the genes were PCR amplified using the specific primer pair (Table 3), and each of the DNA cloned into pET or pQE expression vector.

Overexpression and purification of the His_6-tagged proteins. The bacterial cells were incubated in 100 ml of LB medium at 37℃ with shaking until OD_{600} reached 0.6. Isopropyl-1-thio-β-D-galactopyranoside (IPTG) was then added to a final concentration of 0.5 mM and the growth was continued for 4 h at 37℃. Subsequently, the cells were harvested by centrifugation at 5000 rpm for 10 min, resuspended in buffer A (20 mM Tris-HCl, 500 mM NaCl, 5 mM imidazole, pH 7.9), and the cell suspension disrupted by sonication and then the cell debris removed by centrifugation at 13000 rpm for 10 min. Finally, the His_6-tagged proteins were purified from the supernatant via affinity chromatography using His-Bind resin (Novagen), and the elution was carried out with buffer B (20 mM Tris-HCl, 500 mM NaCl, 1 M imidazole, pH 7.9). Aliquots of the collected fractions were analyzed by SDS-PAGE and the fractions containing most of the purified His_6-tagged kinase were dialyzed against the buffer containing 50 mM sodium phosphate (pH 7.4), 150 mM NaCl, 5 mM $MgCl_2$, and 10% glycerol. The fractions containing His_6-Yor5, His_6-Ugd, His_6-Gnd, His_6-ManC or His_6-ManB were dialyzed against the buffer containing 50 mM Tris-HCl (pH7.5), 100 mM NaCl, 1 mM EDTA, and 10% glycerol.

***In vitro* phosphorylation assay.** The phosphorylation reaction was carried out as described (Grangeasse *et al.*, 2003) by incubating the mixture (20 μl) containing about 2 μg of the purified kinase and/or substrate proteins and 4 μCi (10 μM) [γ-^{32}P]ATP in 25 mM Tris-HCl (pH 7.0), 1 mM DTT, 5 mM $MgCl_2$, 1 mM EDTA at 37℃ for 10 min. The reaction was stopped by addition of the sample buffer and heating at 100℃ for 10 min. After electrophoresis (10% SDS-PAGE), the gel was

visualized by autoradiography with InstantImager^{TM} (Packard Instrument Company) and stained with Coomassie Blue.

Protein dephosphorylation assay. This assay was performed as described (Grangeasse *et al.*, 2003). The purified His_6-tagged proteins were phosphorylated in the presence of [γ-^{32}P] ATP as described above, and then desalted by Microcon YM-10 columns (Millipore) to remove [γ-^{32}P] ATP before dephosphorylation. The dephosphorylation reaction was carried out by adding 1 μg of the purified Yor5 phosphatase with the buffer containing 100 mM sodium citrate (pH6.5) and 1 mM EDTA, and the mixtures were incubated at 37℃ for 30 min. The reaction mixture was stopped and analyzed as described above.

UDP-glucose dehydrogenase assay. The activity of the purified Ugd was determined according to the described spectrophotometric assay (Pagni *et al.*, 1999). The assay was carried out essentially for the purified Ugd, the phosphorylated Ugd, and the dephosphorylated Ugd in the buffer containing 100 mM Tris-HCl (pH 9.0), 100 mM NaCl, 2 mM DTT, 5 mM NAD^+ and 5 mM UDP-glucose and the absorbance at 340 nm was measured by spectrophotometer (Ultrospec 3100 *pro* UV/Visible Spectrophotometer, Amersham Biosciences Ltd).

6-phosphogluconic dehydrogenase assay. The 6-phosphogluconic dehydrogenase activity was determined according to the described assay (Corpas *et al.*, 1998) for the purified Gnd, the phosphorylated Gnd, and the dephosphorylated Gnd in the buffer containing 50 mM Tris-HCl (pH 8.0), 2 mM $MgCl_2$, 2 mM NAD^+ and 2 mM 6-phosphogluconate by measuring absorbance at 340 nm for the formation of NADH.

Results

Part 1: Biological roles of the core elements Wza, Yor5, Yco6, and Wzx encoded in the K2 *cps* gene cluster of *Klebsiella pneumoniae* CG43

Comparative analysis of the *K. pneumoniae cps* gene clusters. In a previous study, *K. pneumoniae* CPS has been shown to be made from a similar biosynthetic pathway to that of *E. coli* group 1 CPS (Whitfield and Roberts, 1999). The sequence of K2 *cps* gene cluster of *K. pneumoniae* Chedid has been determined, which is composed of 19 open reading frames organized into 3 transcriptional units identified (Arakawa *et al.*, 1995). *K. pneumoniae* CG43, as well as *K. pneumoniae* Chedid, produce CPS of K2 serotype (Chang *et al.*, 1996). Comparative analysis of the *cps* gene cluster of *K. pneumoniae* Chedid with that of *E. coli* K30 revealed several conserved genes involved in regulation of high-level polymerization and translocation of CPS, and hence they are called as core elements. These proteins, Wzi, Wza, Yor5, Yco6, Wzx and Wzy, of *K. pneumoniae* Chedid exhibit striking sequence homologies with the proteins, Wzi, Wza, Wzb, Wzc, Wzx and Wzy, of *E. coli* K30 (identity and similarity: 97.6% and 98.4%, 91.0% and 95.5%, 53.1% and 64.6%, 66.5% and 78.3%, 14.1% and 31.4%, 15.9% and 30.3%, respectively). Besides, the genes, *galF*, *orf2*, *gnd* and *manCB*, are also conserved in the two genomes (Fig. 1).

Characterizations of the deletion mutants. In addition to *yor5*$^{-}$ and *yoc6*$^{-}$ mutants, which have been constructed previously (白平輝, 2004), deletion mutations of *wza* and *wzx* were also constructed by using allelic exchange strategy. As shown in Fig. 3 and Fig. 4, Southern blotting analysis using the probes amplified by specific

primer pairs, wzad3 and wzad4 for *wza*$^-$ mutation and wzxM3 and wzxM4 for *wzx*$^-$ mutation, demonstrated that the specific deletions have been introduced. As shown in Fig. 3, 1688-bp signal was detected in the wild type strain and 1238-bp signal was detected in the *wza*$^-$ mutant. Although 2210-bp and 1653-bp signal were detected respectively in wild type strain and *wzx*$^-$ mutant, additional unexpected band was also observed (Fig. 4). The additional unexpected band was about 1800-bp and might be de to incomplete digestion of chromosome or additional deletion of *wzx* homolog. In addition, analysis of Western blotting and RT-PCR indicated that Yco6 protein was not detected in the *yor5*$^-$ mutant and *yco6* mRNA was apparently less than wild type strain (data not shown), suggesting a polar effect of the *yor5* deletion.

Phenotypes of the mutants. Colony morphology of all four mutants appeared to be smaller compared to that of the wild type strain CG43-S3 and the mucoidy was dramatically reduced as determined by string formation (data not shown). As shown in Fig. 5, all the mutants showed higher growth rates than wild type strain in LB broth. In the sedimentation test using a *galU* deletion mutant (U9451) as a negative control, the mutants appeared to precipitate readily, particularly the *wza*$^-$ mutant (Fig. 6). Mucoidy of the *wza* complementing strain appeared to be recovered and the defect in the sedimentation test was also partially restored.

Capsular analysis of the deletion mutants. Since the core elements were assumed to play critical roles in CPS biosynthesis, the defects of these mutants ought to result from modification of CPS biosynthesis. As shown in Fig. 7, the glucuronic acid contents, which serve as indicator of K2 CPS amount (Vodonik and Gray, 1988), of all the mutants were significantly reduced. Furthermore, the CPS purified and analyzed in Fig. 8 showed that all, except the *wza*$^-$ mutant, lost their polymeric CPS, and in turn increased the corresponding oligomeric CPS. In the periplasmic fraction

of the *wza*⁻ mutant, some polymeric CPS were detected indicating that Wza is involved in translocation of polymeric CPS but not in CPS polymerization. Block of the polymeric CPS translocation could feedback-inhibit the upstream CPS biosynthesis and hence resulted in the reduction of total CPS amount. In addition, some polymeric CPS was found in *wzx*⁻ mutant suggesting the existence of an alternative system with low efficiency for the translocation of the CPS oligomer. In the *yor5*⁻ and *yco6*⁻ mutants, disappearance of the high-molecular-weight CPS demonstrated a regulatory role of the tyrosine phosphorylation executed by Yco6 and Yor5 in polymerization of CPS.

Visualization of *K. pneumoniae* CPS by transmission electron microscopy (TEM). The surface-expressed CPS of each of the mutants was labeled with cationized ferritin (Sigma F-7879) as shown in the electron micrograph (Fig. 9), *K. pneumoniae* wild-type strain CG43-S3 appeared to carry an intact thick capsule but the mutants exhibited different levels of unorganized capsules. The disorderly electron-dense materials seen on the surfaces of mutants in micrographs were labeled CPS which might result form dehydration of cells, the treatment for TEM. Notably, the *wza*⁻ mutant had the most smooth surface, and the *wzx*⁻ mutant appeared to carry more of the disrupted CPS on the surface than the other mutants.

Reduction of CPS affected the bacterial susceptibility to polymyxin B and ability of biofilm formation. According to the above mentioned results, deletions of the genes encoding the core elements indeed affected normal CPS expression, but the influences of these defects on bacterial physiology are still not clear. It has been demonstrated in *K. pneumoniae* that increasing amount of CPS and upregulated *cps* transcription were induced by polymyxin B thereby led to the phenotype of polymyxin B resistance (Campos *et al.*, 2004). As shown in Fig. 10, *yor5*⁻ and *wzx*⁻

mutants appeared to be more sensitive to polymyxin B. Capsular expression has been shown to exert significant effect on *K. pneumoniae* biofilm formation (Schembri *et al.*, 2005). Increasing capability of biofilm formation was also observed in either the *yor5*$^{-}$ or the *wzx*$^{-}$ mutant (Fig. 11).

Part 2: Autophosphorylation of protein-tyrosine kinase Yco6 regulates tyrosine phosphorylatoin of the proteins involved in capsular polysaccharide biosynthesis in *Klebsiella pneumoniae* CG43

Tyrosine phosphorylation of Ugd is catalyzed by the cytoplasmic PTK domain of Yco6. Although the tyrosine phosphorylation regulated by PTK and PTP has been shown to modulate biosynthesis and assembly of CPS (Vincent *et al.*, 2000), the mechanism is still unknown. Since the recent reports suggested that *E. coli* Ugd and *B. subtilits* Ugd are the substrates for PTK (Grangeasse *et al.*, 2003; Mijakovic *et al.*, 2003), we herein intend to demonstrate in *K. pneumoniae* CG43 that the Ugd could also be phosphorylated by the PTK, Yco6. In comparing the amino acid sequences of *K. pneumoniae* Ugd (KpUgd) (NTUH-K2044 strain, NCBI accession No. BAD03946) with *E. coli* Ugd (K12 strain, NCBI accession No. NP_416532) and *B. subtilis* YwqF (strain 168, NCBI accession No. CAB15640), approximately 83% and 26% sequence identities were observed respectively. Interestingly, 99.2% amino acid sequence identity was found between KpUgd and the Ugd of *E. coli* K30 strain (NCBI accession No. AAC45348) indicating they are more related. To demonstrate if a similar control of Ugd by PTK Yco6 is present in *K. pneumoniae*, the purified His_6-KpUgd was incubated with the phosphorylated Yco6, His_6-Yco6 (Arg^{451}-Lys^{722}), and [γ-^{32}P] ATP. As shown in Fig. 12A, Yco6 could auto-phosphorylate itself in the presence of [γ-^{32}P] ATP (lane 5) and the phosphorylation of KpUgd could be detected (lane 6) by comparing to the non-radioisotope-labeled His_6-KpUgd while the protein incubated with only [γ-^{32}P] ATP (lane 1). While incubating with the phosphorylated His_6-Wzc (Ser^{447}-Ala^{704}), the PTK of *E. coli* and deleted from its tyrosine cluster, in the presence of [γ-^{32}P] ATP, the His_6-KpUgd appeared to be also phosphorylated (Fig.

12B, lane 2), suggesting that the two PTK, Yco6 and Wzc, exert a similar mechanism via tyrosine phosphorylation to modulate the activity of Ugd.

Phosphorylation enhances the Ugd activity. Ugd is UDP-glucose dehydrogenase catalyzing a NAD^+-dependent transformation of UDP-glucose into UDP-glucuronic acid (Pagni *et al.*, 1999). Phosphorylation of the UDP-glucose dehydrogenases in *E. coli* and *B. subtilis* enhancing their enzymatic activities have recently been reported (Grangeasse *et al.*, 2003; Mijakovic *et al.*, 2003). Consistent with the findings, the enzymatic activity could be enhanced when the recombinant KpUgd was incubated with His_6-Yco6(Arg^{451}-Lys^{722}) and ATP (Fig. 13). When KpUgd was incubated with His_6-Wzc(Ser^{447}-Ala^{704}) and ATP, its activity was also enhanced. In addition, incubation of the phosphorylated His_6-KpUgd with calf intestine alkaline phosphatase (CIAP) (Fermentas) dramatically reduced the Ugd activity, which indicating that phosphorylation of Ugd indeed enhanced its activity, and the purified His_6-KpUgd contained a small fraction of the phosphorylated form.

Tyrosine phosphorylation of either of Gnd, ManC and ManB could be catalyzed by Yco6 and Wzc. In the biosynthesis of *E. coli* group 1 CPS, there are several glycosyltransferases and enzymes, including ManBC and Ugd, involved in the synthesis of sugar nucleotide precursors (Whitfield and Paiment, 2003). Besides, Gnd, a 6-phosphogluconic dehydrogenase, is also required for the formation of the cellular polysaccharide layer (Sprenger, 1995). As shown in Fig. 1, ManBC and Gnd are encoded by the genes in the *cps* gene cluster of *E. coli* and *K. pneumoniae*. The possibility of ManBC and Gnd are also regulated by tyrosine phosphorylation was investigated. When the purified His_6-Gnd, His_6-ManC and His_6-ManB were incubated respectively with [γ-^{32}P] ATP and the phosphorylated His_6-Yco6(Arg^{451}-Lys^{722}), phosphorylations of these proteins were all detected (Fig. 12A, lane 8, 10 and 12)

comparing to those when the proteins incubated only with [γ-^{32}P] ATP (Fig. 12A, lane 2, 3 and 4). When the purified His_6-Gnd, His_6-ManC and His_6-ManB were incubated respectively with [γ-^{32}P] ATP and the phosphorylated His_6-Wzc(Ser^{447}-Ala^{704}), the phosphorylation signals of these proteins were also observed (Fig. 12B, lane 3, 4 and 5). This indicated that phosphorylations of these proteins did not require the tyrosine cluster of PTK.

Phosphorylation of Gnd enhances its 6-phosphogluconic dehydrogenase activity. Gnd is a 6-phosphogluconic dehydrogenase, which catalyzes the oxidative decarboxylation of 6-phospho-gluconate to ribulose-5-phosphate (Sprenger, 1995). When the purified His_6-Gnd was incubated with ATP and either His_6-Yco6(Arg^{451}-Lys^{722}) or His_6-Wzc(Ser^{447} - Ala^{704}), increasing enzymatic activity was observed (Fig. 14). Incubation of the His_6-Gnd with CIAP (Fermentas) also appeared to reduce its activity indicating that the purified His_6-Gnd contained some of the phosphorylated form.

The phosphorylated form of Ugd, Gnd, and ManC could be modified by Yor5. In general, bacteria most often contain antagonistic PTKs and PTPs, and the genes encoding PTKs and PTPs are located next to each other in the same gene clusters. In bacteria, PTK and PTP have been reported to play important roles in regulation of the CPS and EPS production (Nakar and Gutnick, 2003; Stevenson *et al.*, 1996). Many of the PTPs could specifically dephosphorylate the cognate PTKs and also the substrates of PTK (Grangeasse *et al.*, 1998; Mijakovic *et al.*, 2005; Morona *et al.*, 2002; Musumeci *et al.*, 2005; Vincent *et al.*, 1999). To demonstrate if the phosphorylations demonstrated above could be modified specifically by Yor5, aliquots of the purified His_6-Yor5 were added respectively into the above phosphorylation mixtures and incubated at 37℃ for 30 min. As shown in Fig. 12A, the radioactive labels of Gnd

(lane 9) and ManC (lane 11) were removed. On the contrary, no effect on the phosphorylated ManB (lane 13) was found. Interestingly, the phsophorylated KpUgd appeared to be a poor substrate for the recombinant Yor5 (Fig. 12A, lane 7). Moreover, significant amount of Yco6 and Wzc remained to be phosphorylated (Fig. 12A, lane 7, 9, 11, 13, and Fig. 12B, lane 6). I speculate that Yor5 could efficiently remove the phosphorylated tyrosine residues at the C-terminal tyrosine cluster of Yco6. However, the modification at Tyr^{570} which is related to the kinase activity of Yco6 could be low. Therefore, Yor5 would regulate the activity of KpUgd, Gnd, ManC and Yco6 by desphosphorylation. On the other hand, ManB is likely regulated by the other phosphatase.

Discussion

The presence of homologues of Wzi, Wza, Yor5, Yco6, Wzx, and Wzy in *K. pneumoniae* raises the question of whether these proteins are functional conserved. The gene, *wzi*, is only found in the *cps* loci of *K. pneumoniae* and *E. coli* group 1 CPS serotype. Its role in linking high-molecular-weight CPS to cell surface has been demonstrated recently (Alvarez *et al.*, 2000; Rahn *et al.*, 2003). Although the precise way of the linkage is not clear, it is noticeable that *wzi* is confined to the bacteria wherein the capsule is a major virulence factor and their CPS polymers are tightly linked to the cell surface. Wza is assumed to be a multimeric outer membrane protein complex required for surface expression of CPS (Nesper *et al.*, 2003), and *wza*$^-$ mutation in *K. pneumoniae* also showed apparent loss of surface CPS in this study. The block of translocation of polymeric CPS also resulted in reduction of total CPS biosynthesis. The block of translocation of CPS polymer has been suggested to feedback inhibit the upstream CPS biosynthesis, but the exact mechanism remains to be determined (Nesper *et al.*, 2003). As shown in Fig. 6, expression of Wza in *wza*$^-$ mutant could only partially restore the phenotype might result from an inappropriate amount of the expressed protein. Nevertheless, three-dimensional structure of Wza has recently been resolved, which indicated that Wza is an octameric complex with a tetrameric (C4) rotational symmetry and is organized as a tetramer of dimeric subunits (Beis *et al.*, 2004).

Compared with Wza, the studies of Wzx and Wzy are less and confined in O-antigen synthesis, due to the difficulties of purification of the membrane protein and verification of their activities. Some polymeric CPS found in *wzx*$^-$ mutant (Fig. 8) indicated that oligomer could be flipped across inner membrane without Wzx, and

Wzx might not be the only translocator required in the process. The amino sequence of Wzy is variable among strains (identities are less than 16% among *K. pneumoniae* Chedid and NTUH K2044, *E. coli* K12 and K30), and this implies that it is specific to each serotype. So far, no Wzy homolog has been purified and studied at biochemical level to confirm its polymerase activity. In *E. coli* serotype K30 (Drummelsmith and Whitfield, 1999) and K40 (Amor and Whitfield, 1997), *wzy* mutants lack capsules and add only a single K antigen repeat unit to the LPS lipid A core, namely K_{LPS}, implying the role of Wzy for CPS polymerization. Both *yco6* and *yor5* mutants lost high-molecular-weight CPS, suggesting that Yco6 and Yor5 are involved in polymerization of CPS. Overall, mutation in either of the core elements exerted capsule-lacking phenotype. Using the assays of polymyxin B sensitivity and biofilm formation, *yor5* and *wzx* mutants were found to be more susceptible to polymyxin B and increase capability of biofilm formation. Nevertheless, the mechanism is still a question to be investigated.

After thorough analyses, it is believed that PTKs are involved in the regulation of CPS or EPS production (Vincent *et al.*, 2000). The finding that UDP-glucose dehydrogenases are phosphorylated by PTKs strongly supports this viewpoint, although PTKs might play other roles via other mechanisms (Klein *et al.*, 2003; Mijakovic *et al.*, 2006). Herein, we have demonstrated that, in addition to Ugd, Gnd and ManBC are also regulated by tyrosine phosphorylation via Yco6. The phosphorylation appeared also to increase the enzymatic activity, respectively. Although the effect of phosphorylation on ManBC activity has not yet been verified, enhancement of the activity is predictable. Through dephosphorylation by Yor5, the phosphorylated residues is at tyrosine could be inferred. To identify the phosphorylated residue, the amino acid sequences of the enzymes, KpUgd, Gnd and

ManBC, and known substrates of PTK, Ugd and Ssb, were comparatively analyzed. There are 14 to 25 tyrosine residues existing in each protein, however, no conserved motif was found. The phosphorylated site may be determined according to the three-dimensional structure of protein substrate but not specific primary amino acid sequence. In recently, mass spectrometry allowed to pinpoint the phosphorylated tyrosine residue in *B. subtilis* Ssb (Mijakovic *et al.*, 2006), and the phosphorylated residues of KpUgd, Gnd and ManBC might be analyzed by the same method.

Besides the enzymes for CPS precursor synthesis, it is known that the PTKs also autophosphorylate themselves and the phosphorylations at C-terminal tyrosine residues seem to be unrelated to activations of their substrates (Grangeasse *et al.*, 2003). Their kinase activity appeared to be relative to the upstream tyrosine residue and Walker A and B motifs. Moreover, the phosphorylation of the upstream tyrosine and the substrates could not or slowly be dephosphorylated by their cognate PTPs. Only the tyrosine residues in the C-terminal tyrosine cluster of PTKs could be entirely modified by the cognate PTPs implying that different PTP existed to exert the activity to dephosphorylate the upstream tyrosine residue and the tyrosine of certain substrates. The three-dimensional structure of Wzc (Collins *et al.*, 2006) and the finding of the Wza-Wzc interaction (Nesper *et al.*, 2003) indicated that Wzc, as a tetrameric complex with C4 rotational symmetry, forms multienzyme complex with Wza and other membrane proteins which is involved in polymerization and translocation of CPS. The overall level of phosphorylation in the tyrosine cluster is important for capsule assembly, but not the upstream tyrosine (Paiment *et al.*, 2002). Briefly, the PTP-modifiable phosphorylations on the C-terminal tyrosine clusters of PTKs are probably related to conformational changes of PTKs which result in modulating conformation of the multienzyme complex to open or close the translocation channel

of CPS.

As shown in Fig. 15, we propose a model which predicts that Yco6 would regulate both CPS biosynthesis and translocation by phosphorylation. The PTK activity of Yco6 is first enhanced by autophosphorylation at Tyr^{570} and the resulting activation of Yco6 stimulates interphosphorylation at C-terminal tyrosine cluster and also the phosphorylations of its substrates. The phosphorylations of these substrates increase their activities resulting in elevated synthesis of sugar nucleotide precursors. CPS lipid-linked repeat unit composed of sugar nucleotide precursors then is flipped across the inner membrane in a process requiring Wzx and polymerized through Wzy-dependent reaction. Finally, CPS polymer is exported to cell surface via the channel formed by Wza and associated on the surface per the outer membrane protein, Wzi. Although Yco6 also plays roles in CPS polymerization and translocation, it is not yet clear whether these activities require the phosphorylation of Yco6 at specific tyrosine in the C-terminal tyrosine cluster.

References

Alvarez, D., Merino, S., Tomas, J.M., Benedi, V.J., and Alberti, S. (2000) Capsular polysaccharide is a major complement resistance factor in lipopolysaccharide O side chain-deficient *Klebsiella pneumoniae* clinical isolates. *Infect Immun* **68**: 953-955.

Amor, P.A., and Whitfield, C. (1997) Molecular and functional analysis of genes required for expression of group IB K antigens in *Escherichia coli*: characterization of the his-region containing gene clusters for multiple cell-surface polysaccharides. *Mol Microbiol* **26**: 145-161.

Arakawa, Y., Wacharotayankun, R., Nagatsuka, T., Ito, H., Kato, N., and Ohta, M. (1995) Genomic organization of the *Klebsiella pneumoniae cps* region responsible for serotype K2 capsular polysaccharide synthesis in the virulent strain Chedid. *J Bacteriol* **177**: 1788-1796.

Beis, K., Collins, R.F., Ford, R.C., Kamis, A.B., Whitfield, C., and Naismith, J.H. (2004) Three-dimensional structure of Wza, the protein required for translocation of group 1 capsular polysaccharide across the outer membrane of *Escherichia coli*. *J Biol Chem* **279**: 28227-28232.

Bugert, P., and Geider, K. (1997) Characterization of the *amsI* gene product as a low molecular weight acid phosphatase controlling exopolysaccharide synthesis of *Erwinia amylovora*. *FEBS Lett* **400**: 252-256.

Campos, M.A., Vargas, M.A., Regueiro, V., Llompart, C.M., Alberti, S., and Bengoechea, J.A. (2004) Capsule polysaccharide mediates bacterial resistance

to antimicrobial peptides. *Infect Immun* **72**: 7107-7114.

Chang, H.Y., Lee, J.H., Deng, W.L., Fu, T.F., and Peng, H.L. (1996) Virulence and outer membrane properties of a *galU* mutant of *Klebsiella pneumoniae* CG43. *Microb Pathog* **20**: 255-261.

Collins, R.F., Beis, K., Clarke, B.R., Ford, R.C., Hulley, M., Naismith, J.H., and Whitfield, C. (2006) Periplasmic protein-protein contacts in the inner membrane protein Wzc form a tetrameric complex required for the assembly of *Escherichia coli* group 1 capsules. *J Biol Chem* **281**: 2144-2150.

Corpas, F.J., Barroso, J.B., Sandalio, L.M., Distefano, S., Palma, J.M., Lupianez, J.A., and Del Rio, L.A. (1998) A dehydrogenase-mediated recycling system of NADPH in plant peroxisomes. *Biochem J* **330 (Pt 2)**: 777-784.

Domenico, P., Schwartz, S., and Cunha, B.A. (1989) Reduction of capsular polysaccharide production in *Klebsiella pneumoniae* by sodium salicylate. *Infect Immun* **57**: 3778-3782.

Dower, W.J., Miller, J.F., and Ragsdale, C.W. (1988) High efficiency transformation of *E. coli* by high voltage electroporation. *Nucleic Acids Res* **16**: 6127-6145.

Drummelsmith, J., and Whitfield, C. (1999) Gene products required for surface expression of the capsular form of the group 1 K antigen in *Escherichia coli* (O9a:K30). *Mol Microbiol* **31**: 1321-1332.

Duclos, B., Grangeasse, C., Vaganay, E., Riberty, M., and Cozzone, A.J. (1996) Autophosphorylation of a bacterial protein at tyrosine. *J Mol Biol* **259**: 891-895.

Grangeasse, C., Doublet, P., Vaganay, E., Vincent, C., Deleage, G., Duclos, B., and Cozzone, A.J. (1997) Characterization of a bacterial gene encoding an autophosphorylating protein tyrosine kinase. *Gene* **204**: 259-265.

Grangeasse, C., Doublet, P., Vincent, C., Vaganay, E., Riberty, M., Duclos, B., and Cozzone, A.J. (1998) Functional characterization of the low-molecular-mass phosphotyrosine-protein phosphatase of *Acinetobacter johnsonii*. *J Mol Biol* **278**: 339-347.

Grangeasse, C., Obadia, B., Mijakovic, I., Deutscher, J., Cozzone, A.J., and Doublet, P. (2003) Autophosphorylation of the *Escherichia coli* protein kinase Wzc regulates tyrosine phosphorylation of Ugd, a UDP-glucose dehydrogenase. *J Biol Chem* **278**: 39323-39329.

Huang, J., and Schell, M. (1995) Molecular characterization of the eps gene cluster of *Pseudomonas solanacearum* and its transcriptional regulation at a single promoter. *Mol Microbiol* **16**: 977-989.

Hunter, T. (1995) Protein kinases and phosphatases: the yin and yang of protein phosphorylation and signaling. *Cell* **80**: 225-236.

Jayaratne, P., Bronner, D., MacLachlan, P.R., Dodgson, C., Kido, N., and Whitfield, C. (1994) Cloning and analysis of duplicated *rfbM* and *rfbK* genes involved in the formation of GDP-mannose in Escherichia coli O9:K30 and participation of *rfb* genes in the synthesis of the group I K30 capsular polysaccharide. *J Bacteriol* **176**: 3126-3139.

Keen, N.T., Tamaki, S., Kobayashi, D., and Trollinger, D. (1988) Improved

broad-host-range plasmids for DNA cloning in gram-negative bacteria. *Gene* **70**: 191-197.

Klein, G., Dartigalongue, C., and Raina, S. (2003) Phosphorylation-mediated regulation of heat shock response in *Escherichia coli*. *Mol Microbiol* **48**: 269-285.

Lin, W.S., Cunneen, T., and Lee, C.Y. (1994) Sequence analysis and molecular characterization of genes required for the biosynthesis of type 1 capsular polysaccharide in *Staphylococcus aureus*. *J Bacteriol* **176**: 7005-7016.

Manai, M., and Cozzone, A. (1983) Characterization of the amino acids phosphorylated in *E. coli* proteins. *FEMS Microbiol Lett* **17**: 87-91.

Mijakovic, I., Poncet, S., Boel, G., Maze, A., Gillet, S., Jamet, E., Decottignies, P., Grangeasse, C., Doublet, P., Le Marechal, P., and Deutscher, J. (2003) Transmembrane modulator-dependent bacterial tyrosine kinase activates UDP-glucose dehydrogenases. *Embo J* **22**: 4709-4718.

Mijakovic, I., Musumeci, L., Tautz, L., Petranovic, D., Edwards, R.A., Jensen, P.R., Mustelin, T., Deutscher, J., and Bottini, N. (2005) In vitro characterization of the *Bacillus subtilis* protein tyrosine phosphatase YwqE. *J Bacteriol* **187**: 3384-3390.

Mijakovic, I., Petranovic, D., Macek, B., Cepo, T., Mann, M., Davies, J., Jensen, P.R., and Vujaklija, D. (2006) Bacterial single-stranded DNA-binding proteins are phosphorylated on tyrosine. *Nucleic Acids Res* **34**: 1588-1596.

Morona, J.K., Paton, J.C., Miller, D.C., and Morona, R. (2000) Tyrosine

phosphorylation of CpsD negatively regulates capsular polysaccharide biosynthesis in *Streptococcus pneumoniae*. *Mol Microbiol* **35**: 1431-1442.

Morona, J.K., Morona, R., Miller, D.C., and Paton, J.C. (2002) *Streptococcus pneumoniae* capsule biosynthesis protein CpsB is a novel manganese-dependent phosphotyrosine-protein phosphatase. *J Bacteriol* **184**: 577-583.

Musumeci, L., Bongiorni, C., Tautz, L., Edwards, R.A., Osterman, A., Perego, M., Mustelin, T., and Bottini, N. (2005) Low-molecular-weight protein tyrosine phosphatases of *Bacillus subtilis*. *J Bacteriol* **187**: 4945-4956.

Nakar, D., and Gutnick, D.L. (2003) Involvement of a protein tyrosine kinase in production of the polymeric bioemulsifier emulsan from the oil-degrading strain *Acinetobacter lwoffii* RAG-1. *J Bacteriol* **185**: 1001-1009.

Nesper, J., Hill, C.M., Paiment, A., Harauz, G., Beis, K., Naismith, J.H., and Whitfield, C. (2003) Translocation of group 1 capsular polysaccharide in *Escherichia coli* serotype K30. Structural and functional analysis of the outer membrane lipoprotein Wza. *J Biol Chem* **278**: 49763-49772.

Niemeyer, D., and Becker, A. (2001) The molecular weight distribution of succinoglycan produced by *Sinorhizobium meliloti* is influenced by specific tyrosine phosphorylation and ATPase activity of the cytoplasmic domain of the ExoP protein. *J Bacteriol* **183**: 5163-5170.

O'Toole, G.A., and Kolter, R. (1998) Initiation of biofilm formation in *Pseudomonas fluorescens* WCS365 proceeds via multiple, convergent signalling pathways: a

genetic analysis. *Mol Microbiol* **28**: 449-461.

Ørskov, I., and Ørskov, F. (1984) Serotyping of *Klebsiella*. *Methods Microbiol* **14**: 143-164.

Pagni, M., Lazarevic, V., Soldo, B., and Karamata, D. (1999) Assay for UDPglucose 6-dehydrogenase in phosphate-starved cells: gene *tuaD* of *Bacillus subtilis* 168 encodes the UDPglucose 6-dehydrogenase involved in teichuronic acid synthesis. *Microbiology* **145 (Pt 5)**: 1049-1053.

Paiment, A., Hocking, J., and Whitfield, C. (2002) Impact of phosphorylation of specific residues in the tyrosine autokinase, Wzc, on its activity in assembly of group 1 capsules in *Escherichia coli*. *J Bacteriol* **184**: 6437-6447.

Paulsen, I.T., Beness, A.M., and Saier, M.H., Jr. (1997) Computer-based analyses of the protein constituents of transport systems catalysing export of complex carbohydrates in bacteria. *Microbiology* **143 (Pt 8)**: 2685-2699.

Podschun, R., and Ullmann, U. (1998) *Klebsiella* spp. as nosocomial pathogens: epidemiology, taxonomy, typing methods, and pathogenicity factors. *Clin Microbiol Rev* **11**: 589-603.

Preneta, R., Jarraud, S., Vincent, C., Doublet, P., Duclos, B., Etienne, J., and Cozzone, A.J. (2002) Isolation and characterization of a protein-tyrosine kinase and a phosphotyrosine-protein phosphatase from *Klebsiella pneumoniae*. *Comp Biochem Physiol B Biochem Mol Biol* **131**: 103-112.

Rahn, A., Drummelsmith, J., and Whitfield, C. (1999) Conserved organization in the *cps* gene clusters for expression of *Escherichia coli* group 1 K antigens:

relationship to the colanic acid biosynthesis locus and the cps genes from *Klebsiella pneumoniae*. *J Bacteriol* **181**: 2307-2313.

Rahn, A., Beis, K., Naismith, J.H., and Whitfield, C. (2003) A novel outer membrane protein, Wzi, is involved in surface assembly of the *Escherichia coli* K30 group 1 capsule. *J Bacteriol* **185**: 5882-5890.

Reid, A.N., and Whitfield, C. (2005) Functional analysis of conserved gene products involved in assembly of *Escherichia coli* capsules and exopolysaccharides: evidence for molecular recognition between Wza and Wzc for colanic acid biosynthesis. *J Bacteriol* **187**: 5470-5481.

Reuhs, B.L., Geller, D.P., Kim, J.S., Fox, J.E., Kolli, V.S., and Pueppke, S.G. (1998) *Sinorhizobium fredii* and *Sinorhizobium meliloti* produce structurally conserved lipopolysaccharides and strain-specific K antigens. *Appl Environ Microbiol* **64**: 4930-4938.

Schembri, M.A., Blom, J., Krogfelt, K.A., and Klemm, P. (2005) Capsule and fimbria interaction in *Klebsiella pneumoniae*. *Infect Immun* **73**: 4626-4633.

Simoons-Smit, A.M., Verweij-van Vught, A.M., and MacLaren, D.M. (1986) The role of K antigens as virulence factors in *Klebsiella*. *J Med Microbiol* **21**: 133-137.

Sprenger, G.A. (1995) Genetics of pentose-phosphate pathway enzymes of *Escherichia coli* K-12. *Arch Microbiol* **164**: 324-330.

Stevenson, G., Andrianopoulos, K., Hobbs, M., and Reeves, P.R. (1996) Organization of the *Escherichia coli* K-12 gene cluster responsible for production of the extracellular polysaccharide colanic acid. *J Bacteriol* **178**: 4885-4893.

Vincent, C., Doublet, P., Grangeasse, C., Vaganay, E., Cozzone, A.J., and Duclos, B. (1999) Cells of *Escherichia coli* contain a protein-tyrosine kinase, Wzc, and a phosphotyrosine-protein phosphatase, Wzb. *J Bacteriol* **181**: 3472-3477.

Vincent, C., Duclos, B., Grangeasse, C., Vaganay, E., Riberty, M., Cozzone, A.J., and Doublet, P. (2000) Relationship between exopolysaccharide production and protein-tyrosine phosphorylation in gram-negative bacteria. *J Mol Biol* **304**: 311-321.

Vodonik, S.A., and Gray, G.R. (1988) Analysis of linkage positions in a polysaccharide containing nonreducing, terminal alpha-D-glucopyranosyluronic groups by the reductive-cleavage method. *Carbohydr Res* **172**: 255-266.

Wacharotayankun, R., Arakawa, Y., Ohta, M., Hasegawa, T., Mori, M., Horii, T., and Kato, N. (1992) Involvement of *rcsB* in *Klebsiella* K2 capsule synthesis in *Escherichia coli* K-12. *J Bacteriol* **174**: 1063-1067.

Whitfield, C., Perry, M.B., MacLean, L.L., and Yu, S.H. (1992) Structural analysis of the O-antigen side chain polysaccharides in the lipopolysaccharides of *Klebsiella* serotypes O2(2a), O2(2a,2b), and O2(2a,2c). *J Bacteriol* **174**: 4913-4919.

Whitfield, C., and Roberts, I.S. (1999) Structure, assembly and regulation of expression of capsules in *Escherichia coli*. *Mol Microbiol* **31**: 1307-1319.

Whitfield, C., and Paiment, A. (2003) Biosynthesis and assembly of Group 1 capsular polysaccharides in *Escherichia coli* and related extracellular polysaccharides

in other bacteria. *Carbohydr Res* **338**: 2491-2502.

Whitfield, C. (2006) Biosynthesis and Assembly of Capsular Polysaccharides in *Escherichia coli*. *Annu Rev Biochem*.

Zhao, X., and Lam, J.S. (2002) WaaP of *Pseudomonas aeruginosa* is a novel eukaryotic type protein-tyrosine kinase as well as a sugar kinase essential for the biosynthesis of core lipopolysaccharide. *J Biol Chem* **277**: 4722-4730.

白平輝 (2004) 克雷白氏肺炎桿菌 CG43 莢膜多醣體的產生和酪胺酸磷酸化作用的研究. *國立交通大學 生物科技研究所 碩士論文*.

Table 1. Bacterial strains used and constructed in this study

Strain	Genotype or relevant property	Reference or source
***E. coli*:**		
JM109	*RecA1 supE44 endA1 hsdR17 gyrA96 rolA1 thi* △ *(lac-proAB)*	Laboratory stock
NovaBlue(DE3)	*endA1 hsdR17*($rk_{12}^{-}mk_{12}^{+}$) *supE44 thi-1 recA1 gyrA96 relA1 lac*[F′ *pro AB* lac^{q}Z△M15:: Tn*10*](DE3);Tet^{r}	Novagen
BL21-RIL	F^{-} *ompT* $hsdS_B(r_B^{-}m_B^{-})$*gal dcm*(DE3)	Laboratory stock
S17-1 λ*pir*	Tp^{R} Sm^{R} *recA, thi, pro,* $hsdR^{-}M^{+}$ [RP4-2-Tc::Mu:Km^{r}Tn*7*] (*pir*)	De Lorenzo *et al.*, 1994
M15(pREP4)	Nal^{S}, Str^{S}, Rif^{S}, Thi^{-}, Lac^{-}, Ara^{+}, Gal^{+}, Mtl^{-}, F^{-}, $RecA^{+}$, Uvr^{+}, Lon^{+}	Qiagen
***K. pneumoniae*:**		
CG43	Clinical isolate of K2 serotype	Laboratory stock
CG43-S3	*rspl* mutant, $Strep^{R}$	Laboratory stock
CG43-S3-U9451	*galU* deletion mutant	Laboratory stock
CG43-S3-*wza*$^{-}$	*wza* deletion mutant in CG43-S3	This study
CG43-S3-*yor5*$^{-}$	*yor5* deletion mutant in CG43-S3	白平輝, 2004
CG43-S3-*yco6*$^{-}$	*yco6* deletion mutant in CG43-S3	白平輝, 2004
CG43-S3-*wzx*$^{-}$	*wzx* deletion mutant in CG43-S3	This study
***P. aeruginosa*:**		
PAO1	Non-mucoid *P. aeruginosa* strain O1	Laboratory stock

Table 2. Plasmids used and constructed in this study

Plasmid	Description	Reference or source
pKAS46	Suicide vector, Amp^R, Km^R	Laboratory stock
pRK415	Shuttle vector, *mob*$^+$, Tc^R	Laboratory stock
pKAS46-*wza*$^-$	A 2.0-kb fragment containing a 500-bp deletion in *wza* locus cloned into pKAS46, Amp^R, Km^R	This study
pKAS46-*yor5*$^-$	A 2.0-kb fragment containing a 150-bp deletion in *yor5* locus cloned into pKAS46, Amp^R, Km^R	白平輝, 2004
pKAS46-*yco6*$^-$	A 2.0-kb fragment containing a 1800-bp deletion in *yoc6* locus cloned into pKAS46, Amp^R, Km^R	白平輝, 2004
pKAS46-*wzx*$^-$	A 2.0-kb fragment containing a 600-bp deletion in *wzx* locus cloned into pKAS46, Amp^R, Km^R	This study
pKAS46-*wzy*$^-$	A 2.0-kb fragment containing a 1200-bp deletion in *wzy* locus cloned into pKAS46, Amp^R, Km^R	This study
pRK415-Wza	pRK415 derivative carrying *wza* on an *Kpn* Ⅰ /*Bam*H Ⅰ fragment, Tc^R	This study
pRK415-Yor5	pRK415 derivative carrying *yor5* on an *Eco*R Ⅰ/ *Eco*R Ⅰ fragment, Tc^R	This study
pRK415-Yco6	pRK415 derivative carrying *yco6* on an *Bam*H Ⅰ/ *Bam*H Ⅰ fragment, Tc^R	This study
pRK415-Wzx	pRK415 derivative carrying *wzx* on an *Bam*H Ⅰ/ *Bam*H Ⅰ fragment, Tc^R	This study
pRK415-Wzy	pRK415 derivative carrying *wzy* on an *Hind*Ⅲ/ *Bam*H Ⅰ fragment, Tc^R	This study
pET-30a-c	Overexpression of His_6 fusion proteins, Km^R	Novagen
pQE30-32	Overexpression of His_6 fusion proteins, Amp^R	Qiagen
pET30-Yco6E23	Encoding Yco6 from Arg^{451} to Lys^{722}, His_6–Yco6(Arg^{451}-Lys^{722}), cloned in *Eco*R Ⅰ/*Sal* Ⅰ sites, Km^R	This study
pET30-Yor5	Encoding Yor5 from Met^1 to Ala^{144}, His_6–Yor5, cloned in *Eco*R Ⅴ/*Sac* Ⅰ sites, Km^R	白平輝, 2004
pET30-Ugd	Encoding KpUgd from Met^1 to Asp^{388}, His_6–KpUgd, cloned in *Eco*R Ⅰ/*Sal* Ⅰ sites, Km^R	白平輝, 2004
pET30-Gnd	Encoding Gnd from Met^1 to Glu^{468}, His_6–Gnd, cloned in *Bam*H Ⅰ/*Sac* Ⅰ sites, Km^R	白平輝, 2004
pQE31-ManC	Encoding ManC from Met^1 to Cys^{471},	This study

	His_6–ManC, cloned in *Bam*HⅠ/*Hin*dⅢ sites, Amp^R	
pQE31-ManB	Encoding ManB from Met^1 to Lys^{468}, His_6–ManB, cloned in *Bam*HⅠ/*Hin*dⅢ sites, Amp^R	This study
pQE30-41	Overexpression of His_6–Wzc(Ser^{447}-Lys^{720}), Amp^R	Grangeasse *et al*., 2003
pQE30-42	Overexpression of His_6–Wzc(Ser^{447}-Ala^{704}), Amp^R	Grangeasse *et al*., 2003
pQE30-U	Overexpression of His_6–Ugd(Lys^2-Asp^{388}), Amp^R	Grangeasse *et al*., 2003

Table 3. Primers used in this study

Primer	Sequence (5' to 3')
WzaD1	TTTCTATGGGCAGATGGTTG
WzaD2	CAGAATTCACCCAGTTACCG
WzaD3	CCGCAGTGGTATGACAATTG
WzaD4	GCTGACTATCGGGAAGCATC
Yor5D1	GGTTGGCGATATCTTAATGG
Yor5D2	GCTGATTGGTGAGCTCCATG
Yor5D3	CGAAGCACGAGCTCAGACA
Yor5D4	AATCGCTCCGGACCATTGGC
Yco6D1	GCTGACTGGCGATATCTTGTGT
Yco6D2	CACCAACCAATCGATCAAAGTC
Yco6D3	GCATAATCGATTGGCGGAATTA
Yco6D4	CTCCTTCTGGAGCTCGTTTTCA
WzxD1	TCGATATCGCTATATTGACAACC
WzxD2	AGAAAGCTTAATCTATCCAGCC
WzxD3	CTGCAAAGCTTGGTTTATGCA
WzxD4	CTGATAGATGAGCTCTGGAATG
WzyD1	CAACCATGGAGCTCGATTAGATAT
WzyD2	GCAGTCGACTTATATTATGCATGTC
WzyD3	CGAAAATGACGTCGACTAAAGTTA
WzyD4	GTTTGCTACCATACGCATTGCT
WzaE1	CACC AAGAAAAAAATTGTTAGATTTTCG
WzaE2	CTAAACATATTATGGCCAATCC
Yor5E1	CTCCATTGGTTCGTTGGAAT
Yor5E2	GCATTCGCTTGTTTCTGTTC
Yco6N1	CTGGATCCCAGGAAATAATGCATGACTTC
Yco6N2	CACTGCAGGTCCCCTTCTTGAGTAACCT
Yco6E2	CGTAAAGGAATTGAAACTCCAGA
Yco6E3	AAGGGGATTCTTCGTCCCCT
WzxN1	CTGGATCCGCGAAGGTATTACTAGATGAGT
WzxN2	CACTGCAGATGATTTGGCAGCATATTTA
WzyE1	CACCATTCGAAGAAAGTTTTCTCG
WzyE2	CTTTAGTTGATGTCATTTTCG
UgdE1	CGAATGAAAATTACTATTTCCGG
UgdE2	CCAGTGTCAGACAGGCAGAA
GndE1	GACCACACCAGACAGGAGCAAGT
GndE2	CTCGGGCGGCATATAAAGA

ManCE1	CACCTTGCTTCCTGTGATTATGGC
ManCE2	TCTGCGATTTGTCCCGAA
ManBE1	ATGGTCGTTGCTAATTTTTTCG
ManBE2	GGCTTCCATTATGGATAATGC

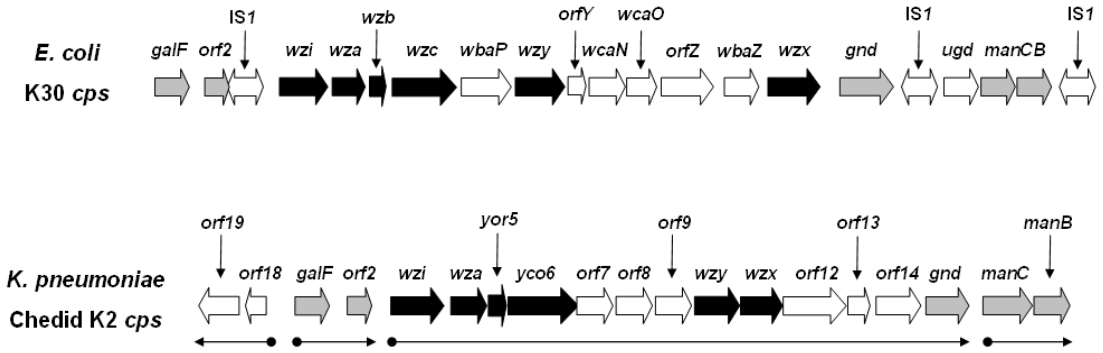

Fig. 1. **The comparison of *cps* gene clusters.** The gene clusters encoding capsular polysaccharide in *E. coli* and *K. pneumoniae* Chedid are shown (Whitfield and Paiment, 2003; Arakawa *et al*., 1995). The genes coding for core elements are marked solid black, and the conserved genes are marked with gray color. The underline arrows represent the putative transcriptional units in the *K. pneumoniae cps* region.

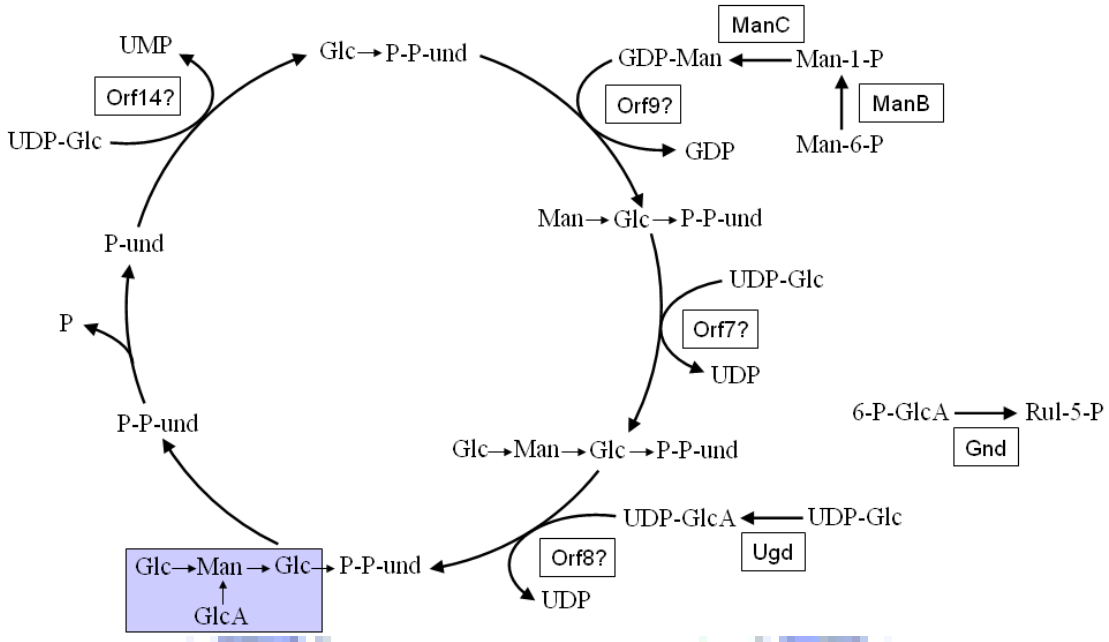

Fig.2. **Biosynthesis pathway of lipid-linked K2 repeat units.** This diagram shows the proposed pathway for synthesis of lipid-linked K2 repeat units. The assignment of glycosyltransferases catalyzing individual steps is based on sequences and functions analysis with those of *E. coli* K30 (Whitfield and Paiment, 2003). Enzymes and glycosyltransferases involved in the synthesis of sugar nucleotide precursor are identified by boxes. Ugd is UDP-glucose dehydrogenase, and ManBC are phosphomannomutase and GDP-mannose pyrophosphorylase, respectively. Und-P is undecaprenyl phosphate which is supposed to be a carrier lipid.

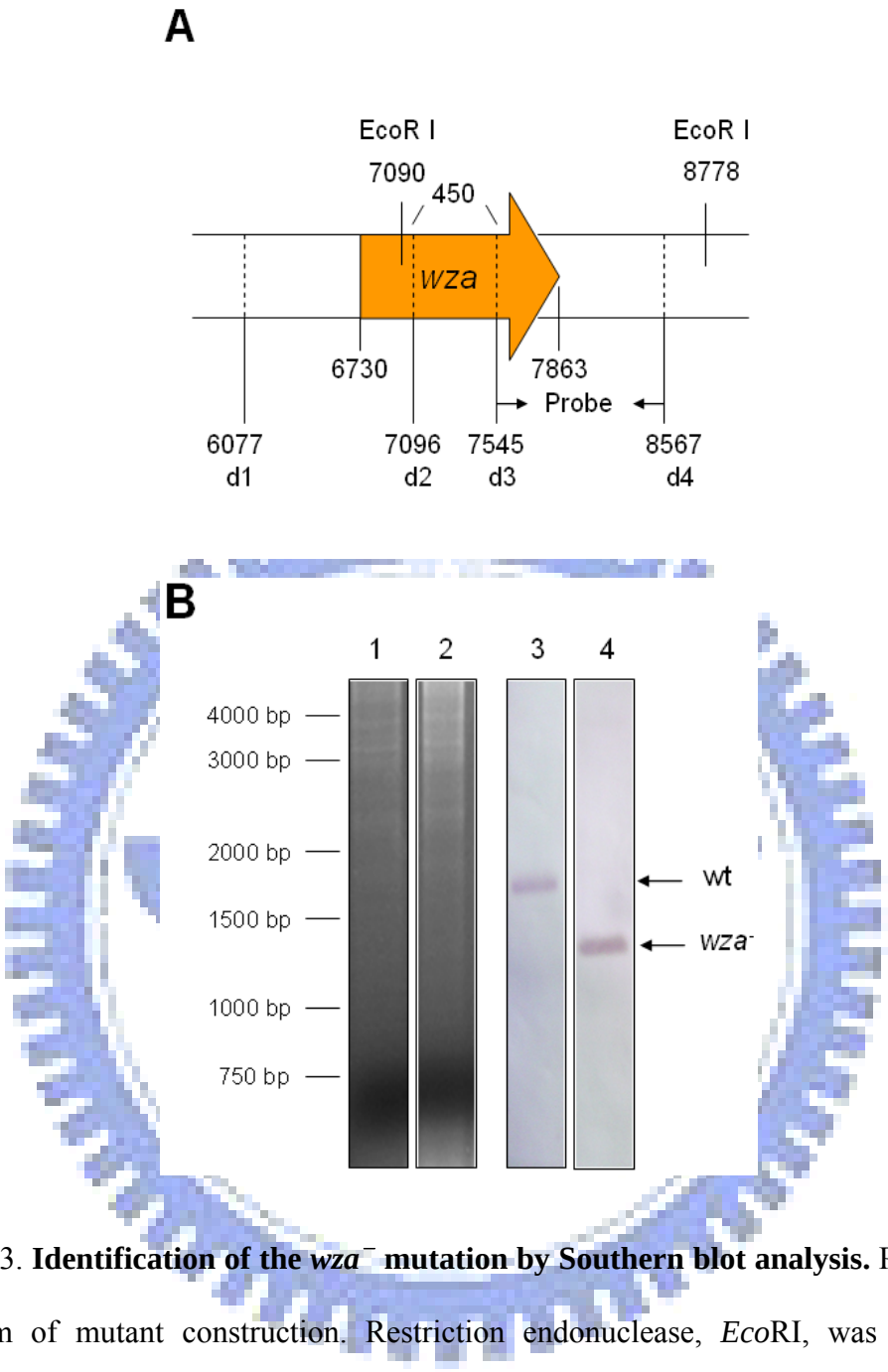

Fig. 3. **Identification of the *wza*⁻ mutation by Southern blot analysis.** Panel A is diagram of mutant construction. Restriction endonuclease, *Eco*RI, was used for chromosome digestion, and the numbers indicate the sites in Chedid *cps* gene cluster. Panel B, PCR product using wzad3 and wzad4 primer pair was used as probe of Southern blot analysis. Lane 1, photograph of ethidium bromide-stained gel of wild type strain *K. pneumoniae* CG43-S3; lane 2, photograph of ethidium bromide-stained gel of *wza*⁻ mutant; lane 3, photograph of Southern blot of wild type strain *K. pneumoniae* CG43-S3; lane 4, photograph of Southern blot of *wza*⁻ mutant.

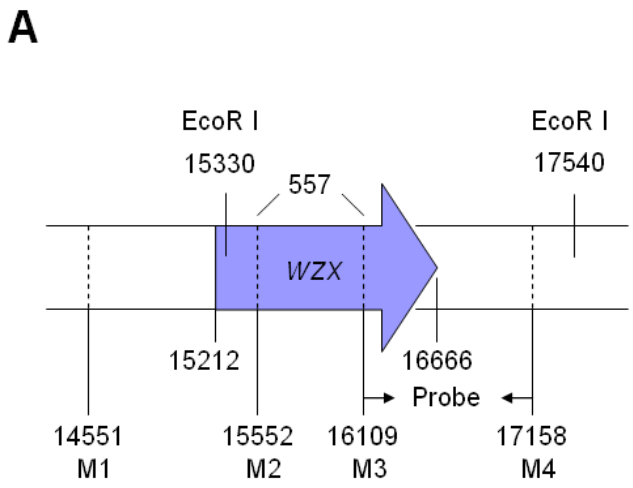

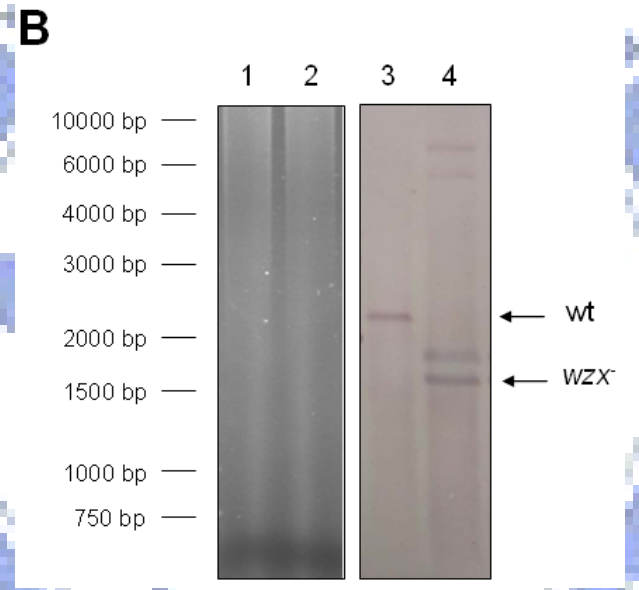

Fig. 4. **Identification of the *wzx*⁻ mutation by Southern blot analysis.** Panel A is diagram of mutant construction. Restriction endonuclease, *Eco*RI, was used for chromosome digestion, and the numbers indicate the sites in Chedid *cps* gene cluster. Panel B, PCR product using wzxM3 and wzxM4 primer pair was used as probe of Southern blot analysis. Lane 1, photograph of ethidium bromide-stained gel of wild-type strain *K. pneumoniae* CG43-S3; lane 2, photograph of ethidium bromide-stained gel of *wzx*⁻ mutant; lane 3, photograph of Southern blot of wild type strain *K. pneumoniae* CG43-S3; lane 4, photograph of Southern blot of *wzx*⁻ mutant.

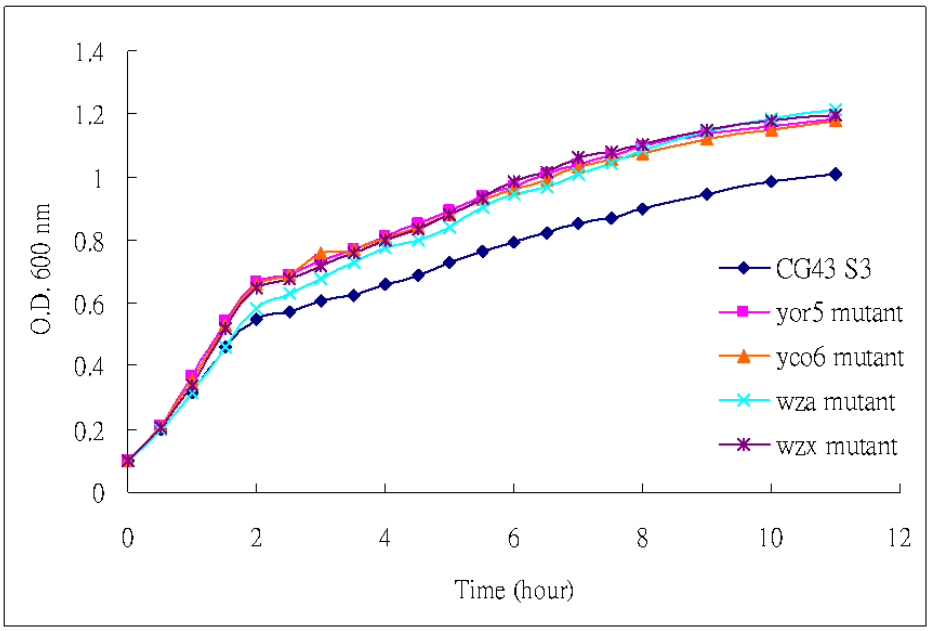

Fig. 5. **Mutants grow faster than wild type strain.** Growth curves of the bacteria of wild type strain *K. pneumoniae* CG43-S3, *wza*$^{-}$, *yor5*$^{-}$, *yco6*$^{-}$ and *wzx*$^{-}$ at 37℃ in LB broth.

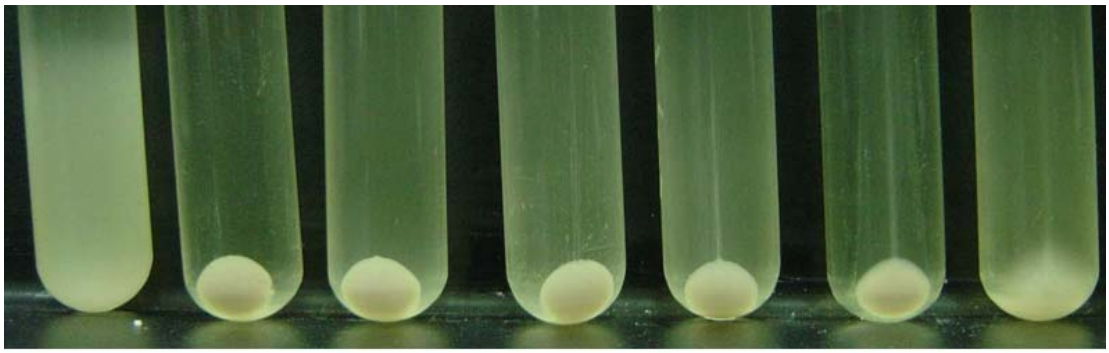

Fig. 6. **Loss of colony mucoidy – Sedimentation test.** Overnight cultures of wild-type strain *K. pneumoniae* CG43-S3, *wza*⁻, *yor5*⁻, *yco6*⁻, *wzx*⁻, *galU*⁻ and the *wza* complement were subjected to 3000 rpm centrifugation for 3 min.

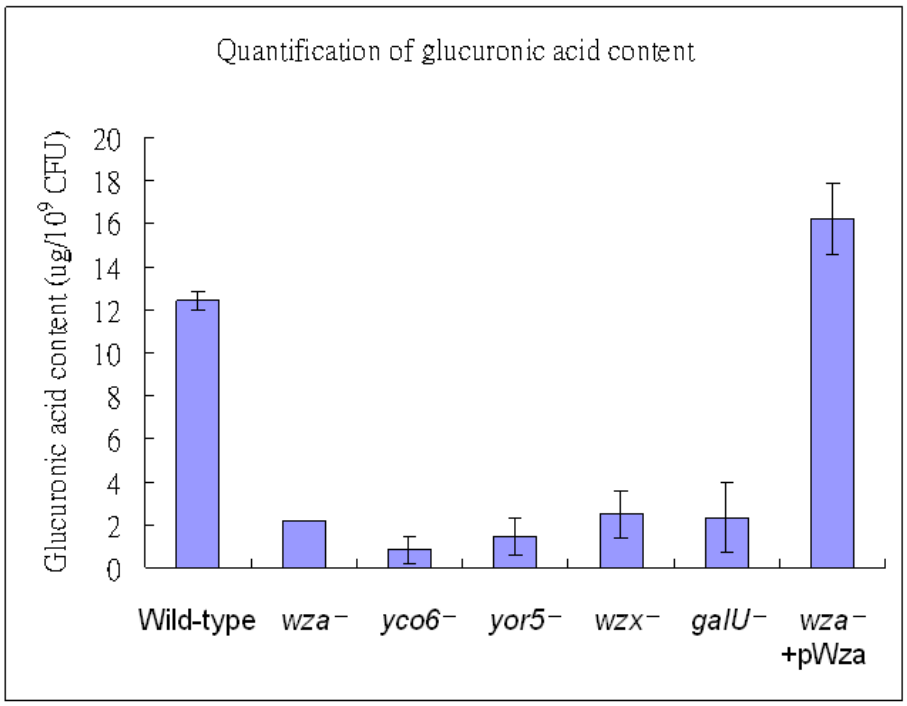

Fig. 7. **Reduction of the glucuronic acid content.** The bacterial CPS from 500 μl of overnight culture was extracted and then hydrolyzed by H_2SO_4, and 3-hydroxydiphenol was added to measure the absorbance at 520 nm. Glucuronic acid was used as a standard for the quantification of uronic acid.

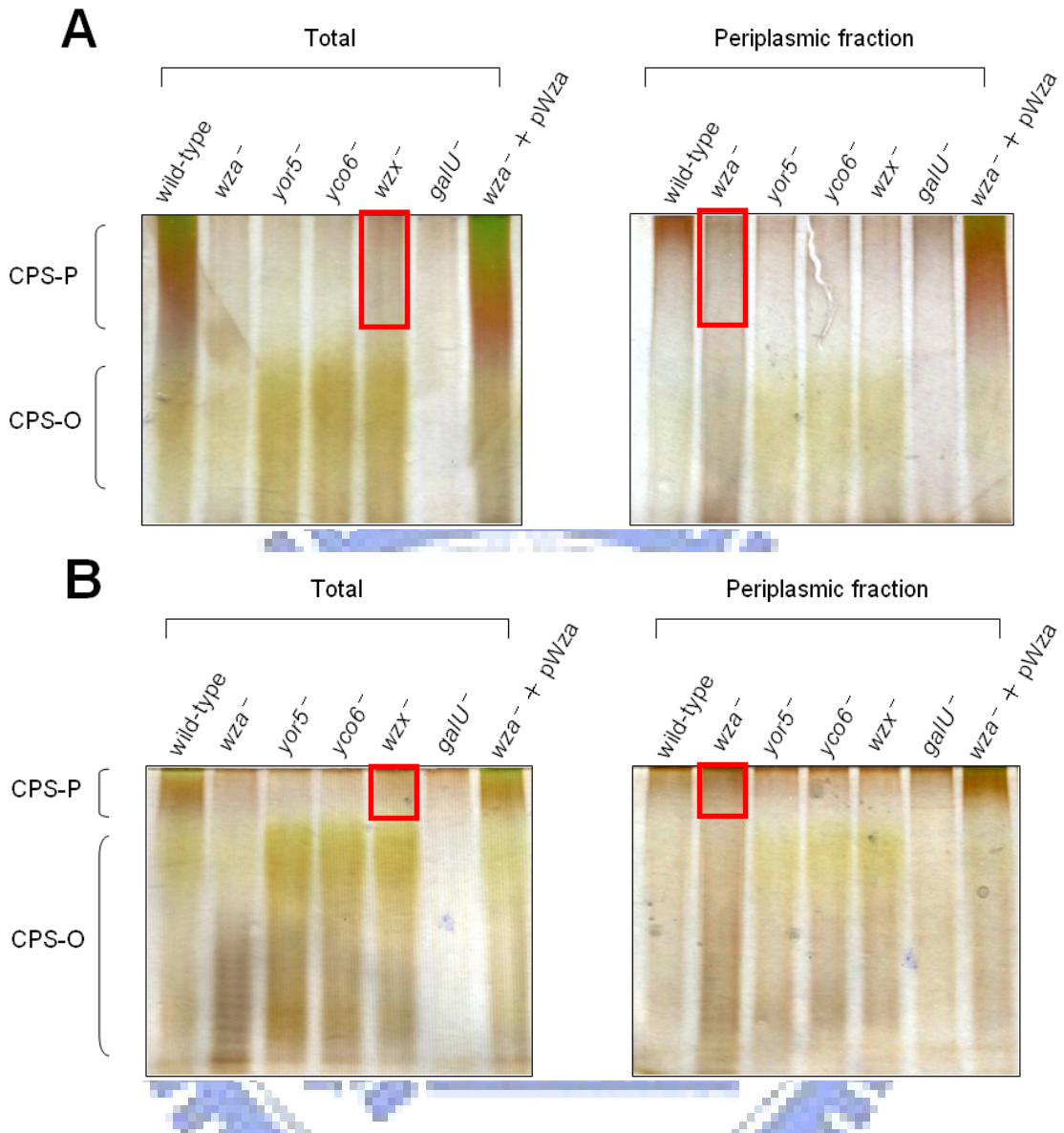

Fig. 8. **Alterations of capsular polysaccharides.** Overnight cultured bacteria were harvested, and the CPS purified by hot phenol extraction (total) or osmotic shock (periplasmic fraction).After treatments with DNase, RNase and proteinase K and dialysis against water, the CPS were analyzed on (A) 5% DOC-PAGE and (B) 10% DOC-PAGE followed by alcain blue-silver staining. (Reuhs et *al*., 1998) CPS-P: high-molecular-weight polymeric CPS; CPS-O: low-molecular-weight oligomeric CPS. The frames represent the detectable polymeric CPS in the *wzx*⁻ mutant and the periplasmic fraction of the *wza*⁻ mutant.

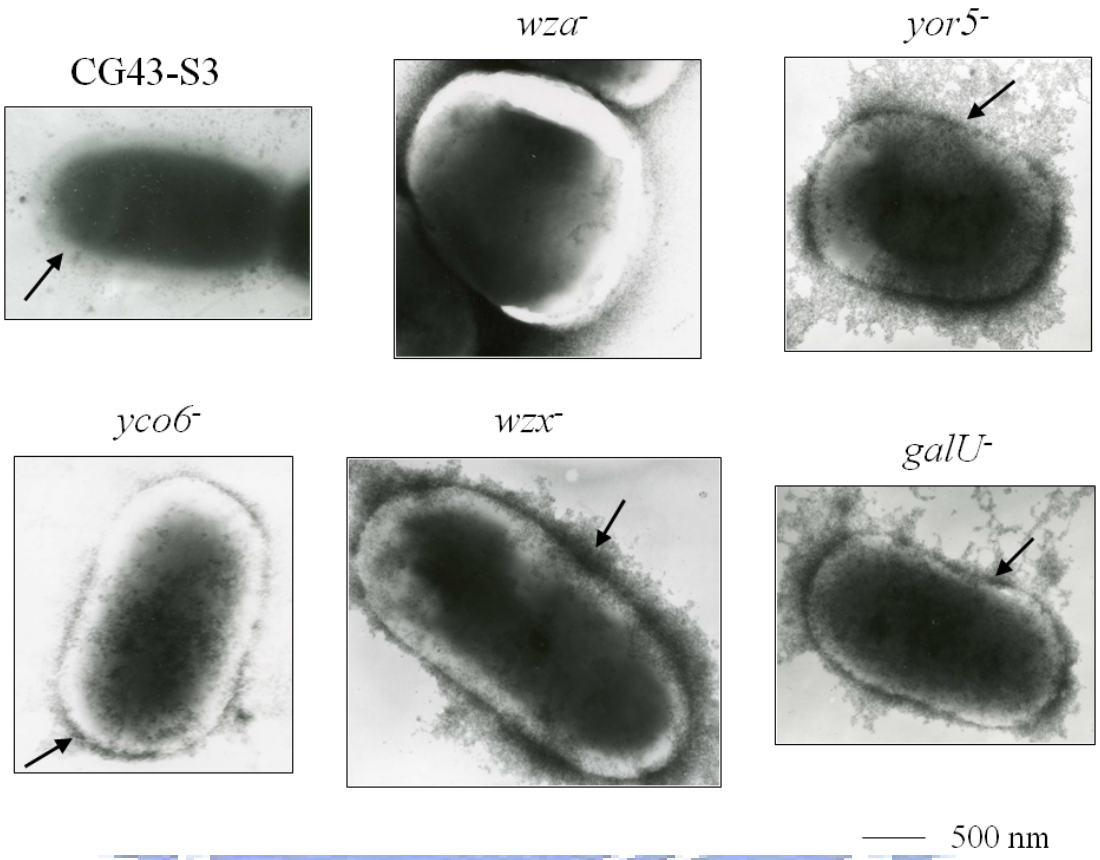

Fig. 9. **Electron micrographs of *K. pneumoniae*.** The micrographs of wild type strain *K. pneumoniae* CG43-S3, *wza*$^-$, *yor5*$^-$, *yco6*$^-$, *wzx*$^-$ and *galU*$^-$ show the effects of respective mutation on surface-expressed CPS. The surface-expressed CPS was labeled with cationized ferritin and the micrographs of TEM were taken at Chang Gung University, Taiwan. The arrows indicate the stained CPS, and no CPS expressed on surface in *wza*$^-$ mutant.

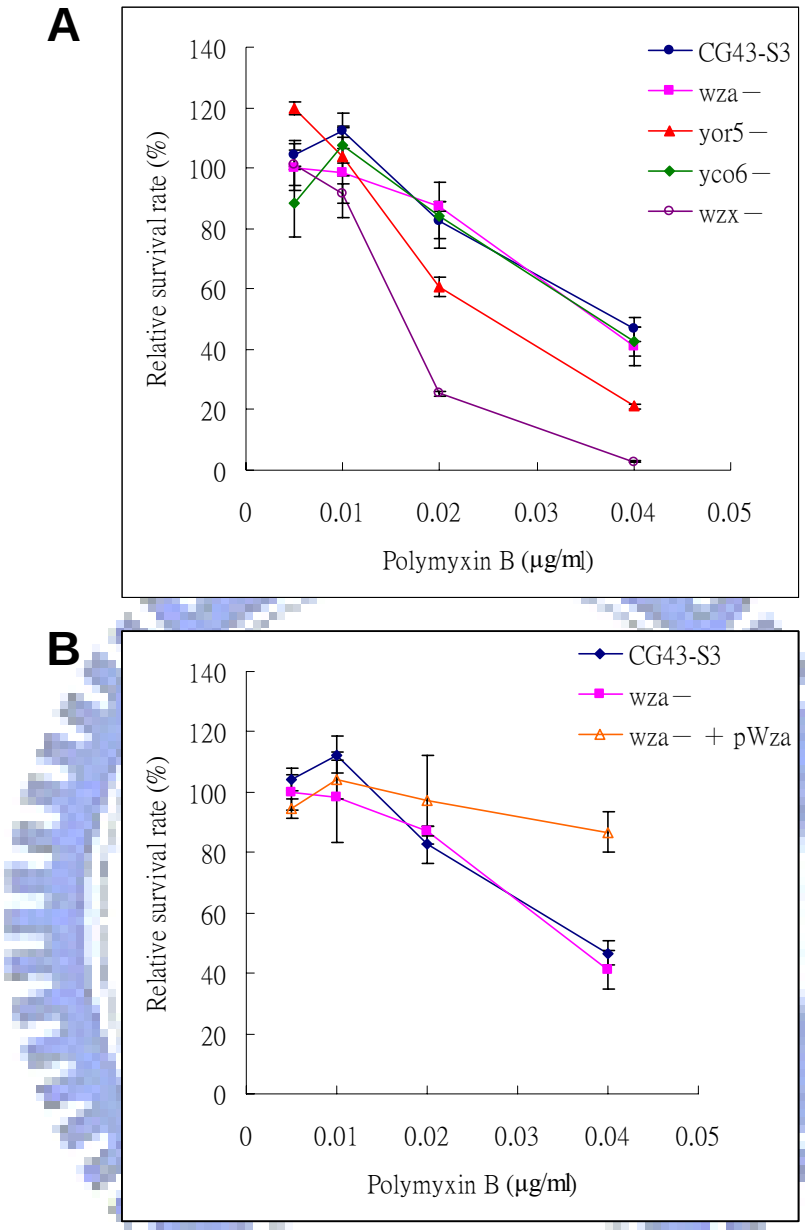

Fig. 10. **Effects of the susceptibility to polymyxin B.** Bacteria were harvested in the exponential phase of growth, and resuspended in 1% (wt/vol) tryptone-PBS (pH 7.4). Survival bacteria (percentage of colony counts of cell not exposed to polymyxin B) were counted by incubation with different amounts of polymyxin B at 37℃ for 30 min. Each point represents the mean of three samples and the vertical lines show the standard deviations. The relationships among wild-type CG43-S3 and (A) mutants or (B) overexpression of Wza in *wza*$^{-}$ mutants were shown.

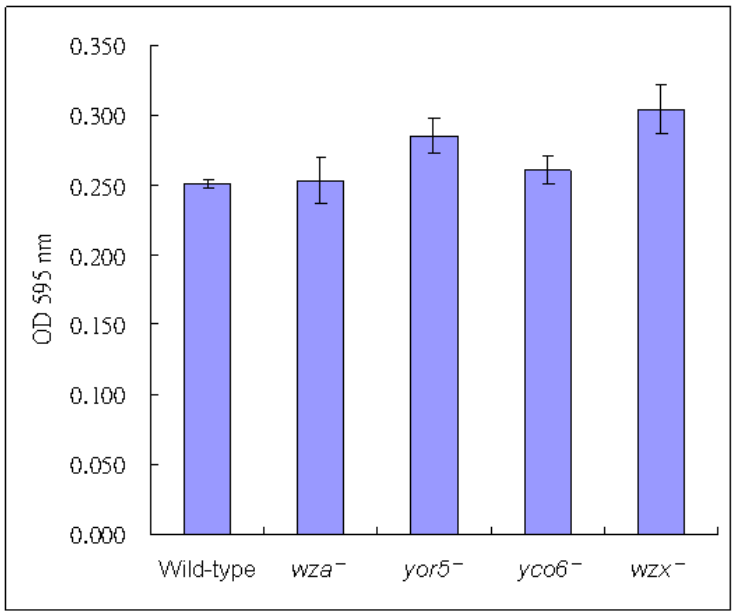

Fig. 11. **Biofilm formation ability.** Overnight cultured bacteria were 100-fold diluted, and incubated in 96-well microtiter dish at 37℃ for 48 hours. After stained by 1% crystal violet, the absorbance was determined at 595 nm. Each bar represents the mean of three samples and vertical line indicates the standard deviation.

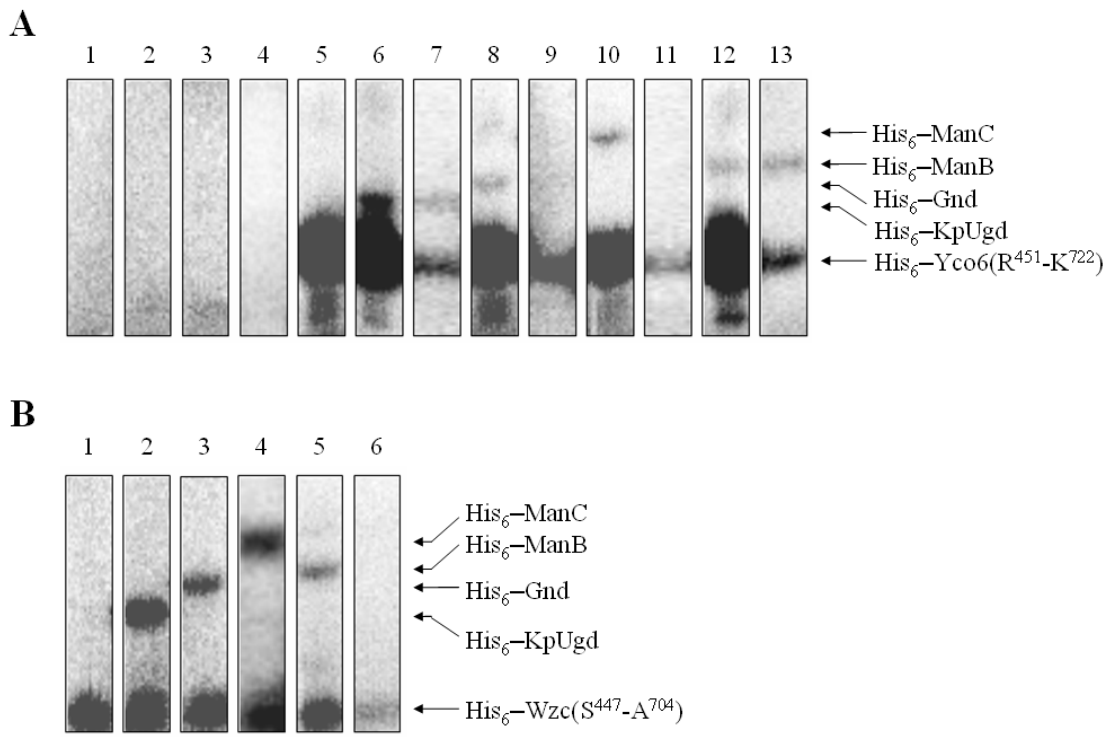

Fig. 12. ***In vitro* phosphorylation and dephosphorylation of different proteins**. Autoradiography of *in vitro* phosphorylation and dephosphorylatoin assays separated on SDS-PAGE. The lanes contained reaction mixtures and [γ-^{32}P] ATP with the following proteins: **(A)** His_6-KpUgd (lane 1), His_6-Gnd (lane 2), His_6-ManC (lane 3), His_6-ManB (lane 4), His_6-Yco6(Arg^{451}-Lys^{722}) (lane 5), His_6-Yco6(Arg^{451}-Lys^{722}) and His_6-KpUgd (lane 6), His_6-Yco6(Arg^{451}-Lys^{722}), His_6-KpUgd and His_6-Yor5 (lane 7), His_6-Yco6(Arg^{451}- Lys^{722}) and His_6-Gnd (lane 8), His_6-Yco6(Arg^{451}- Lys^{722}), His_6-Gnd and His_6-Yor5 (lane 9), His_6-Yco6(Arg^{451}-Lys^{722}) and His_6-ManC (lane 10), His_6-Yco6(Arg^{451}- Lys^{722}), His_6-ManC and His_6-Yor5 (lane 11), His_6-Yco6(Arg^{451}-Lys^{722}) and His_6-ManB (lane 12), His_6-Yco6(Arg^{451}-Lys^{722}), His_6-ManB and His_6-Yor5 (lane 13). **(B)** His_6-Wzc(Ser^{447}-Ala^{704}) (lane 1), His_6-Wzc(Ser^{447}-Ala^{704}) and His_6-KpUgd (lane 2), His_6-Wzc(Ser^{447}-Ala^{704}) and His_6-Gnd (lane 3), His_6-Wzc (Ser^{447}-Ala^{704}) and His_6-ManC (lane 4), His_6-Wzc(Ser^{447}-Ala^{704}) and His_6-ManB (lane 5), His_6-Wzc (Ser^{447}-Ala^{704}) and His_6-Yor5 (lane 6).

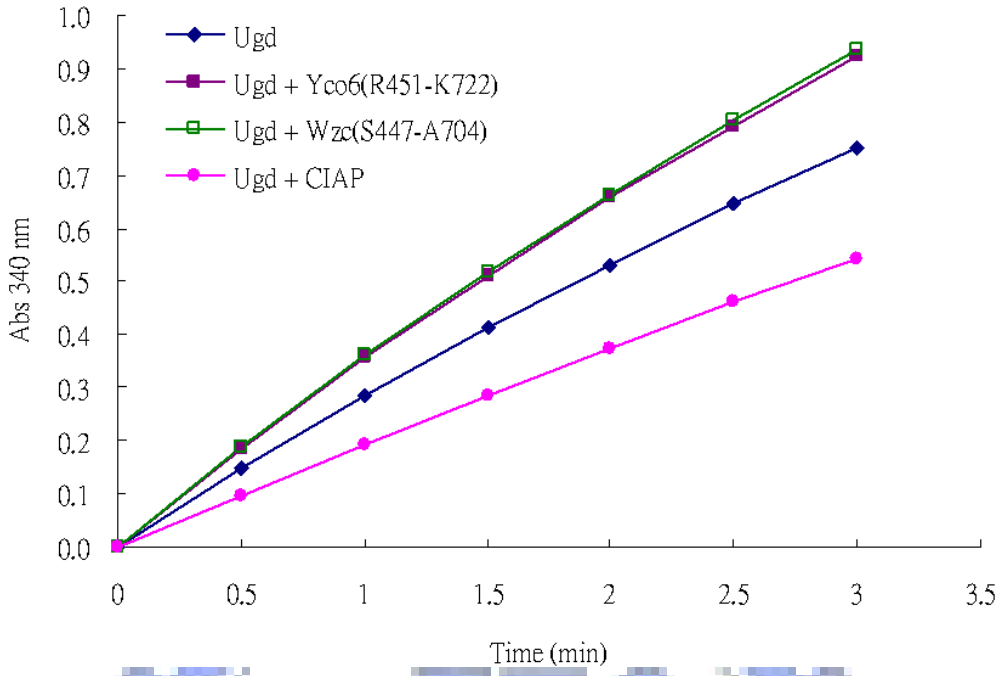

Fig. 13. **Phosphorylation of Ugd enhances its UDP-glucose dehydrogenase activity.** UDP-glucose dehydrogenase activity was monitored at 340 nm for 3 min by measuring NADH formation in the mixture containing His_6-KpUgd (◆), His_6-KpUgd previously phosphorylated by His_6-Yco6(Arg^{451}-Lys^{722}) (■), His_6-KpUgd previously phosphorylated by His_6-Wzc(Ser^{447}-Ala^{704}) (□), His_6-KpUgd previously treated with calf intestine alkaline phosphatase (CIAP) (●). All the contents of proteins used here were 5 μg each.

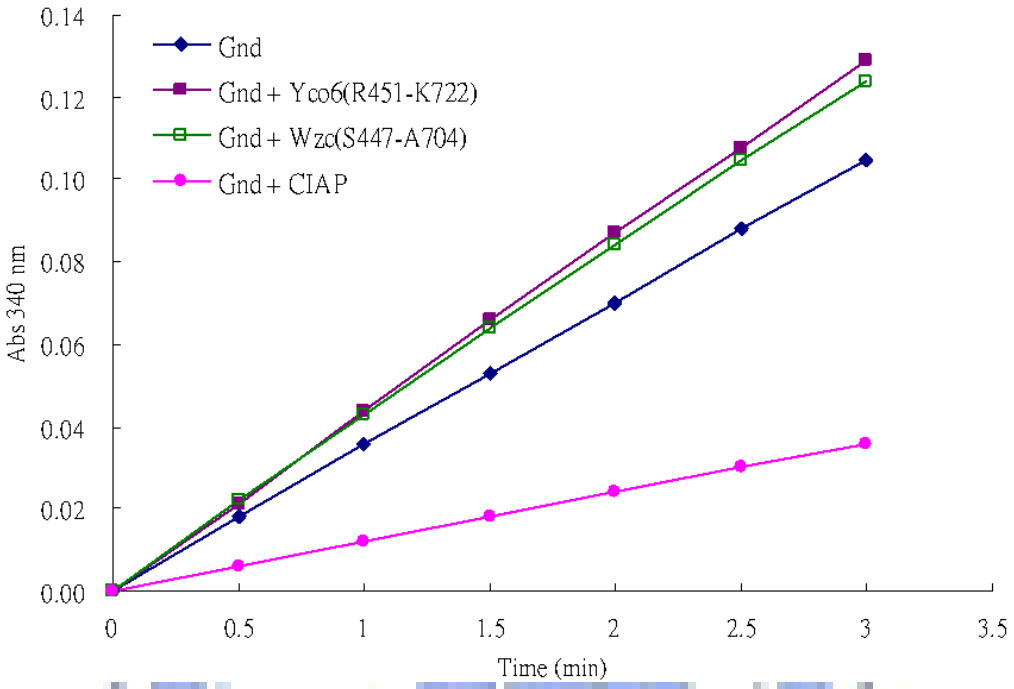

Fig. 14. **Phosphorylation of Gnd enhances its 6-phosphogluconic dehydrogenase activity.** UDP-glucose 6-phosphogluconic dehydrogenase activity was monitored at 340 nm for 3 min by measuring NADH formation in the mixture containing His_6-Gnd (◆), His_6-Gnd previously phosphorylated by His_6-Yco6(Arg^{451}-Lys^{722}) (■), His_6-Gnd previously phosphorylated by His_6-Wzc(Ser^{447}-Ala^{704}) (□), His_6-Gnd previously treated with calf intestine alkaline phosphatase (CIAP) (●). All the contents of proteins used here were 5 μg each.

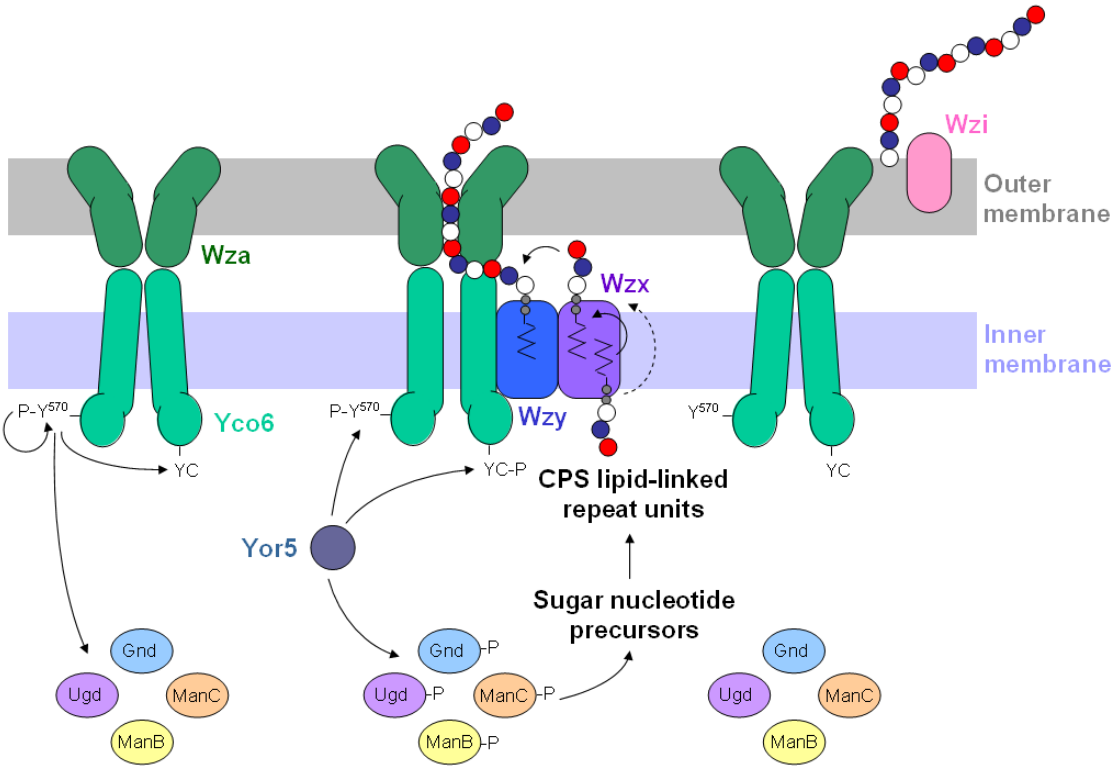

Fig. 15. **Schematic model for functional roles of core elements involved in CPS biosynthesis in *K. pneumoniae*.** Beginning at the left, Yco6 catalyzes autophosphorylation on Tyr^{570} and interphosphorylation on C-terminal tyrosines (marked as YC in figure). The substrates, Ugd, Gnd and ManBC, are also phosphorylated by autophosphorylated Yco6 and result in enhancing their enzyme activities to produce sugar nucleotide precursors. CPS lipid-linked repeat units are synthesized by utilizing sugar nucleotide precursors, and then flipped across the membrane in a process requiring Wzx. These repeats units are polymerized through Wzy-dependent polymerization. The phosphorylation on Yco6 C-terminal tyrosines might cause its conformational change which likely affects the protein-protein interaction of Yco6 with other proteins in the multienzyme complex and regulates polymerization and translocation of CPS. Yor5 would control above reactions by dephosphorylation. Wza acts as a channel to translocate CPS polymers, and Wzi appears to be involved in modulating surface association.

Appendix 1. Features of the ORFs encoded in Chedid K2 *cps* region from *K. pneumoniae*.

ORF	Signal peptide predicated	Putative protein name	Putative transmembrane regions	Putative function	Organism	% identity/ % positives	Accession No.
Orf1	N	GalF	1	UTP-glucose-1-phosphate uridylyltransferase	*E. coli*	98/99	AAN52283
Orf2	Y	N/A	6	Acid phosphatase homologues	*K. pneumoniae*	95/97	BAD86766
Orf3	Y	Wzi	1	Protein for surface expression of capsule	*E. coli*	97/99	AAD21561
Orf4	Y	Wza	1	Putative outer membrane lipoprotein	*E. coli*	91/96	AAD21562
Orf5	N	Yor5	0	Protein-tyrosine-phosphatase	*K. pneumoniae*	100/100	Q48451
Orf6	N	Yco6	2	Protein-tyrosine kinase	*K. pneumoniae*	100/100	Q48452
Orf7	N	CpsG	1	Putative glycosyltransferase	*B. xenovorans*	31/52	YP_553596
Orf8	N	N/A	0	Putative glycosyltransferase	*E. coli*	28/44	AAV74375
Orf9	N	N/A	0	Putative mannosyltransferase	*A. actinomycetemcomitans*	37/54	BAA94398
Orf10	N	Wzy	10	Repeat unit polymerase	*E. coli*	16/30	AAD21566
Orf11	N	Wzx	12	Putative export protein, flippase	*E. coli*	45/65	NP_288552
Orf12	Y	N/A	3	Hypothetical 65.4 kDa protein in *cps* region	*K. pneumoniae*	100/100	Q48458
Orf13	N	WcjD	0	Putative acetyltransferase	*S. pneumoniae*	25/39	CAI33033
Orf14	N	RfbP	4	Putative glycosyltransferase	*K. pneumoniae*	79/85	BAD86780
Orf15	N	Gnd	1	6-phosphogluconate dehydrogenase	*K. pneumoniae*	100/100	P41576
Orf16	N	ManC	0	Mannose-1-phosphate guanylyltransferase	*K. pneumoniae*	100/100	Q48462
Orf17	N	ManB	0	Phosphormannonutase dehydrogenase	*K. pneumoniae*	98/99	BAD03945
Orf18	N	YegH	4	Putative transmembrane protein	*K. pneumoniae*	99/99	BAD86764
Orf19	N	YegH	2	Putative transmembrane protein	*K. pneumoniae*	97/98	BAD86764

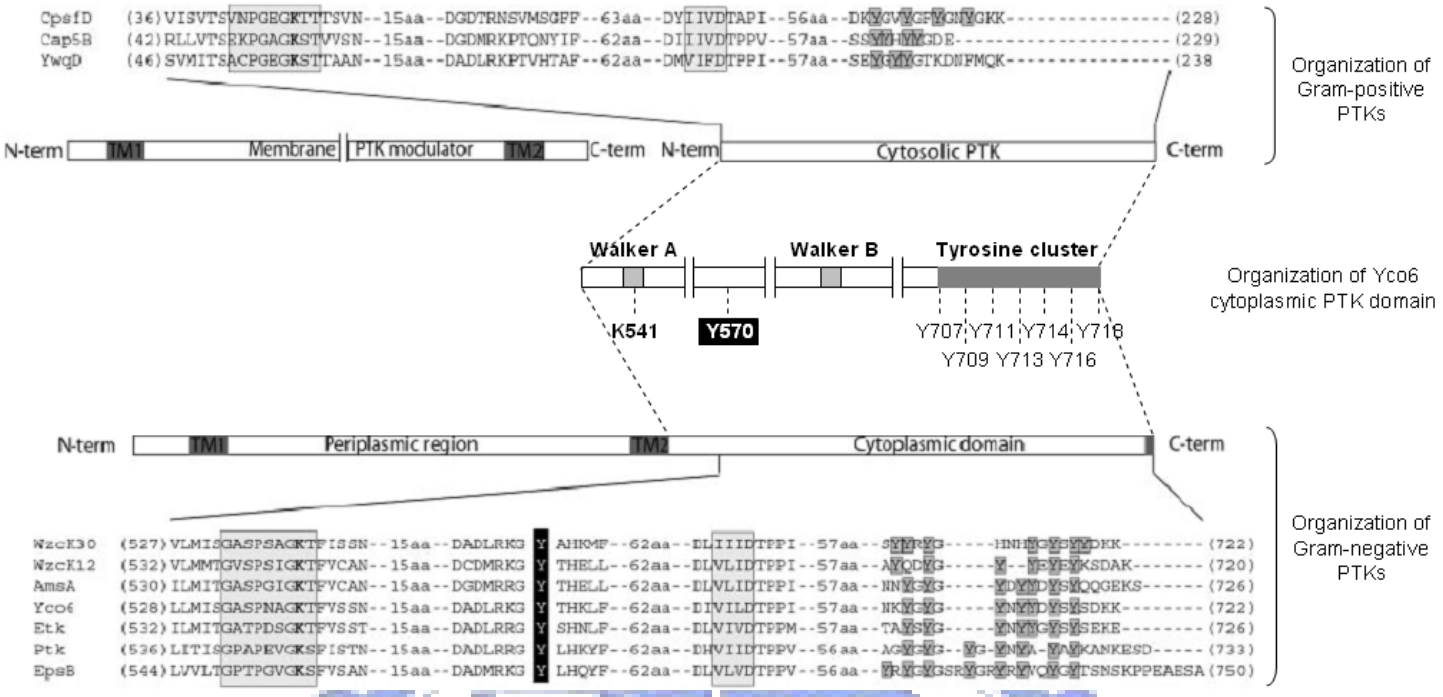

Apendix 2. **Sequence alignment and structural features of bacterial PTKs.** The PTK cytoplasmic domain of Yco6 from *K. pneumoniae* K2 serotype is presented in the middle section. The structural comparison of Gram-positive (top section) and Gram-negative (bottom section) PTKs is presented. The C-terminal cytosolic PTK domain is enlarged, and sequence alignment of PTKs from Gram-positive bacteria (*S. pneumoniae* Cps19fD, *S. aureus* Cap5B, and *B. subtilis* YwqD) and Gram-negative bacteria (*E. coli* K30 Wzc, *E. coli* K12 Wzc, *E. amylovora* AmsA, *K. pneumoniae* Yco6, *E. coli* E2348/69 Etk, *A. johnsonii* Ptk, and *Rastonia solanacearum* EpsB) was performed by using the Vector NTI program (InforMax, Inc.). The Walker A and B ATP-binding motifs are indicated as light gray shaded boxes, the two predicted transmembrane α-helices of the PTKs termed TM1 and TM2, are indicated by dark shaded boxes, tyrosine residues of the tyrosine cluster are in gray boxes, and Tyr^{570} is in black box. Dashes indicate gaps introduced in the alignment process.